NTNU
Norwegian University of
Science and Technology

Modelling of variable speed centrifugal compressors for anti-surge control

Per Aaslid

Master of Science in Engineering Cybernetics
Submission date: June 2009
Supervisor: Tor Arne Johansen, ITK
Co-supervisor: Jørgen Spjøtvold, ABB
Bjørnar Bøhagen, ABB

Norwegian University of Science and Technology
Department of Engineering Cybernetics

Problem Description

Anti-surge control is an important issue in operation of oil and gas processing plants. Both with respect to operability and environmental issues. For example, every processing platform in the North Sea have several such controllers. However, it seems to be little, if any, focus on the control theoretic properties of such controllers. This thesis is about supporting the closing of this gap by establishing a sufficiently good process model for control strategy validation.

1. Review existing models relevant for anti-surge control validation
2. Derive a dynamic model for a simple compression system including
   a. Upstream pressure vessel, for which the feed is a system input
   b. Gas cooler, for which cooling medium temperature and flow are system inputs
   c. Compressor scrubber
   d. Compressor
   e. Downstream compressor pressure vessel including check valve, for which the outflow is system input
   f. Recycle line from compressor output to gas cooler including the anti-surge valve, for which valve openings are system inputs
   g. Governor - Gas turbine
3. Implement model in Simulink
4. Validate model with data experienced at installations

Assignment given: 12. January 2009
Supervisor: Tor Arne Johansen, ITK

Summary

A mathematical model for simulation of gas compressor systems is developed. The model is designed for anti-surge control validation, and models a continuous flow gas compressor. The model also includes a cooler for gas cooling, a scrubber for liquid draining, and a recycle line with a control valve for anti-surge control. The system outlet has a check valve to prevent reversed flows. The model is one-dimensional and models pressure, temperature and mass flow for all system components, and also compressor shaft speed. It is modular and derived using mass, momentum and energy balance. Compressor characteristics maps from compressor manufacturer are used to determine compressor pressure ratio, efficiency and shaft power. The model also includes upstream and downstream systems, which are modelled as large vessels with very slow dynamics. In addition, a model structure for gas turbine, which can be used as compressor governor, has been proposed.

The mathematical model has been implemented in Simulink® and verified against experimental data from an oil and gas installation. The simulations give good fit with the dataset. Simulations also show that the dynamics at the compressor inlet and outlet is dominated by the large volumes, mainly the upstream and downstream vessel, while the faster dynamics are damped out.

Preface

This report presents the work done in my master thesis at the department of Engineering Cybernetics at the Norwegian University of Science and Technology, spring 2009. The thesis is accomplished in cooperation with ABB Process Automation, Advanced Solutions in Oslo.

Modelling thermodynamics is not my special field, and it has been challenging to crack the physical system down to differential equations, but through my studies I have learned how to split a complex problem in to smaller less complex problems. This work has given me a new understanding of oil and gas installations, especially compressors and gas turbines. Even though I have not seen the equipment I have been modelling physically, the gap between theory and practice have been reduced thanks to ABB, who have supplied specification and dataset experienced at installations.

During my studies I have visited ABB in Oslo three times for guidance and feedback. I am grateful to my advisors Dr Jørgen Spjøtvold and Dr Bjørnar Bøhagen at ABB, who have followed up my work weekly through phone meetings. Jørgen has helped me to find relevant literature and documentations for my work, and he has also given me good feedback concerning thesis writing. Bjørnar's expertise has been very helpful for my understanding of compressors. I am thankful to Dr Olav Slupphaug and Erik Roald at ABB, who have shared their expertise and experience within compressor systems and gas turbines. I would also like to thank my supervisor Prof Tor Arne Johansen for advice regarding Matlab® and thesis writing. Finally, I would like to thank my fellow student Terje Kvangardsnes, who also has worked with compressors, for good cooperation and useful discussions.

Trondheim, June 2009 Per Aaslid

Contents

List of Figures

List of Tables

Nomenclature

$\bar{R} = 8.314$ Universal gas constant $\left[\frac{m^2 mol}{s^2 kgK}\right]$

η	Efficiency $[.]$
κ	Specific heat ratio $\frac{c_p}{c_v}$ $[.]$
ω	Rotational speed $[s^{-1}]$
ρ	Denisty $\left[\frac{kg}{m^3}\right]$
τ	Momentum $[Nm]$
A	Area $[m^2]$
C	Velocity $\left[\frac{m}{s}\right]$
c_p	Specific heat constant pressure $\left[\frac{J}{kgK}\right]$
c_v	Specific heat constant volume $\left[\frac{J}{kgK}\right]$
E	Energy $[J]$
e	Energy per unit mass $\left[\frac{J}{kg}\right]$
H	Enthalpy $[J]$
h	Specific enthalpy $\left[\frac{J}{kg}\right]$
HHV	Higher Heating Value $\left[\frac{J}{kg}\right]$
J	Inertia $[kgm^2]$
L	Lenght $[m]$
l	Valve stroke position $[\%]$
M	Molar weight $\left[\frac{kg}{mol}\right]$
m	Mass $[kg]$
N	Compressor speed $[rpm]$
P	Power $[W]$
p	Pressure $[Pa]$

p_c	Critical pressure $[Pa]$
Q	Heat $[J]$
q	Volume flow $\left[\frac{m^3}{h}\right]$
$R = \frac{\bar{R}}{M}$	Specific gas constant $\left[\frac{m^2}{s^2 K}\right]$
T	Temperature $[K]$
t	Time $[sec]$
T_c	Critical temperature $[K]$
U	Internal energy $[J]$
u	Specific internal energy $\left[\frac{J}{kg}\right]$
UH	Heat transfer coefficient $\left[\frac{W}{m^2 K}\right]$
V	Volume $[m^3]$
W	Work $[J]$
w	Mass flow $\left[\frac{kg}{s}\right]$
z	Compressibility factor $[.]$

1 Introduction

1.1 Motivation

Compressors are widely used both on- and off-shore for gas processing and transportation. Oil rigs and gas processing plants have several compressors operating either alone, in trains or in parallels. To maximize profit, the compressors should be controlled to give a high production, but also as low as possible power consumption. Compressors have a limited working range with respect to gas flow. A high flow reduces the compressor pressure ratio and it will at some point choke. One the other hand, a too low flow can cause surge and rotating stall. Surge is a phenomena characterized by oscillations in flow and pressure, while stall is characterized by locally reduced or blocked flow. Note that stall is a phenomenon inside the compressor, and the flow upstream and downstream the compressor is not necessarily affected. A more detailed description of these phenomena are available in Gravdahl and Egeland (1998, p. 14-20).

There are two approaches to handle surge and rotating stall, active control and avoidance. Active control aims at stabilizing surge and rotating stall while avoidance, which is also known as anti-surge control, ensures that the system operates in stable regions (Bøhagen, 2007, p. 2-3). In this thesis we will focus on surge avoidance.

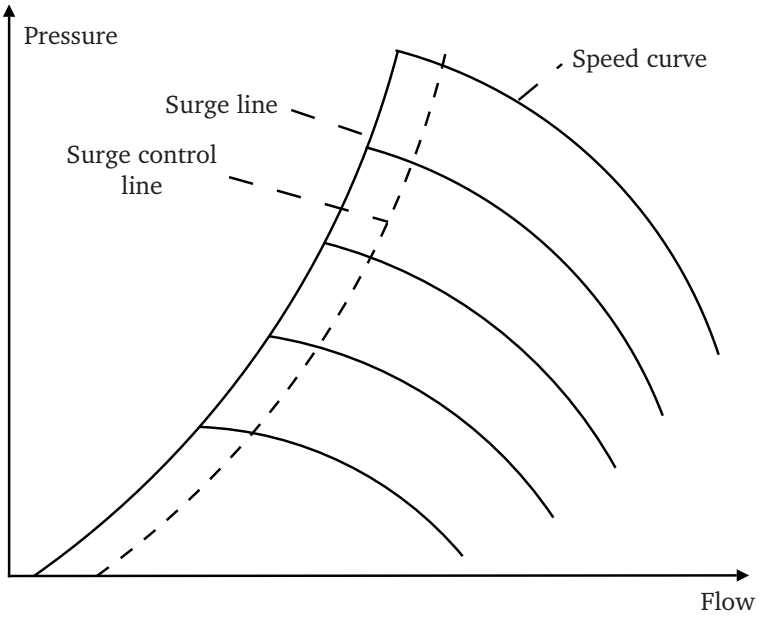

Figure 1.1: Compressor characteristics chart.

Figure 1.1 shows a typical compressor chart where the compressor outlet pressure is represented as a function of flow on the x-axis and compressor speed represented with the parallel curves. For a given compressor there will exist a surge line, which gives the flows and speeds the compressor will enter surge. The surge control line defines a boundary for which region the anti-surge controller should allow the compressor to operate in. The area on the right side of the surge control line is stable. As seen on the figure, there is a safety margin between the surge line and surge control line.

To avoid surge, compressors are equipped with a recycle line, which can recycle compressed gas back into the compressor again. An anti-surge controller is used to control the recycle flow through a recycle valve. This solution permits the compressor to maintain high enough flow to not enter surge even if the flow into the system is below the limit for the current pressure ratio. However, this is not optimal with respect to energy consumption since some of the gas is compressed twice. This approach is implemented on industrial compressors worldwide and is a safe and reliable method. Due to the consequences of failure, anti-surge controllers are conservative with respect to safety margins. By reducing these margins power consumption can also be reduced, which yet again will increase the profit and also reduce the emissions.

The objective of this thesis is to make a modular dynamic model of a compressor and its surrounding process equipment. The purpose of the model is to validate different anti-surge control strategies, and the model should be complex enough to simulate behaviour relevant for this objective. A equivalent model will also be made for the compressor governor, which in this case is driven by a gas turbine drive.

Previous scientific work covers modelling of all the involved components separately, but not assembled into a similar system to the one described here and not for this purpose. As mentioned above, the model should be complex enough for this purpose, hence some of the previous models have to be either simplified or extended depending on how dominating they are in the overall system. The previous work that will be used in this thesis is cited when used in the modelling section.

The compressor and the surrounding equipment are characterized by complex non-linear behaviour, and designing a safe and efficient controller is extremely difficult. A change in recycle flow will change both pressure and temperature upstream to the compressor, which yet again will affect the flow. An increased flow will increase the compressor power consumption, which yet again can affect the drive and the compressor speed. In addition the drive might have complex dynamics, which also affects the system. The dynamics in a compressor system is clearly complex and it is difficult analyse the consequences of a change in any of the system inputs or boundary conditions.

The possibilities of testing an anti-surge controller on a full scale compressor are limited because of the consequences of failure. A compressor running in surge is hazardous for the environment and can cause severe damages. In other words, experimenting with anti-surge controllers for large industrial compressors is both risky and expensive. Therefore, we want to design a simulator of the compressor and its surrounding equipment that enables us to study dynamics when there is a change in the recycle flow, the compressor inlet temperature, the system inlet flow or maybe a fault somewhere in the system. The simulator allows us to test new anti-surge controllers and strategies easily and inexpensive.

1.2 Contributions of this thesis

A gas compression system modelled in this thesis consists of:

- Compressor for gas compression.
- Scrubber for liquid removal.
- Cooler for gas cooling.
- Recycle line for gas recycle back into compressor.
- Check valve to prevent reversed flows at system outlet.
- Upstream vessel to represent upstream process.
- Downstream vessel to represent downstream process.
- Governor for the compressor with either an electrical drive or a gas turbine.

The behaviour of each component depends on pressure, flow and temperature from upstream and downstream components together with ambient conditions. Each component is modelled as independent modules using mass, flow and energy balance. Further, they have been interconnected to represent the desired system. This method allows for rearranging the modules to represent different industrial solutions. It is also possible to simulate compressor trains if desirable. The gas turbine and its modules have been modelled equivalent.

The modules are implemented and assembled in Simulink®. To identify and validate system parameters, simulation results have been compared with experienced data from a gas compressor at a gas processing plant, which henceforth will be called Plant A. Finally, the model is evaluated to state its usefulness with

respect to anti-surge control validation, analyzing and testing. The gas turbine model has been assembled similarly and initialized using steady state values from a processing plant called Plant B.

1.3 Overview of this thesis

A brief description of the modelled system, its components and functionality is presented in Section 2. Some basic thermodynamic properties that will be used in this thesis are also introduced here. Section 3 describes mathematical modelling of the system, and in Section 4 the system is identified and validated. In Section 5 the system is evaluated, and the conclusions and future work is presented in Section 6.

2 Theory

This section presents background information, physical properties and assumption for the modelling in Section 3. In Section 2.1 the compressor and turbine system configuration is described, while Section 2.2 describes each system component individually. Section 2.3-2.8 introduces models and terms for further use, and discuss some of the assumptions made in the modelling.

2.1 System description

2.1.1 Compressor system

A typical compressor system is shown in Figure 2.1. The upstream vessel represents an upstream process equivalent, and is fed with a mass flow. From the upstream vessel, the flow is lead into the cooler. The cooling medium flow is controlled with a controller, which seeks to keep the processing gas outflow temperature constant. After the cooling, liquid is removed from the gas in the scrubber before entering the compressor. The pressure is increased through the compressor, and a recycle line at the compressor outlet allows recycling of the processing gas back to the cooler to maintain a high enough flow through the compressor. The fraction of the flow that is not recycled leaves the system through the check valve into the downstream vessel that represents the downstream process. The check valve prevents reversed flow from the downstream vessel into the compressor. The recycle line has a control valve called the anti-surge valve that is controlled with the anti-surge controller. This controller

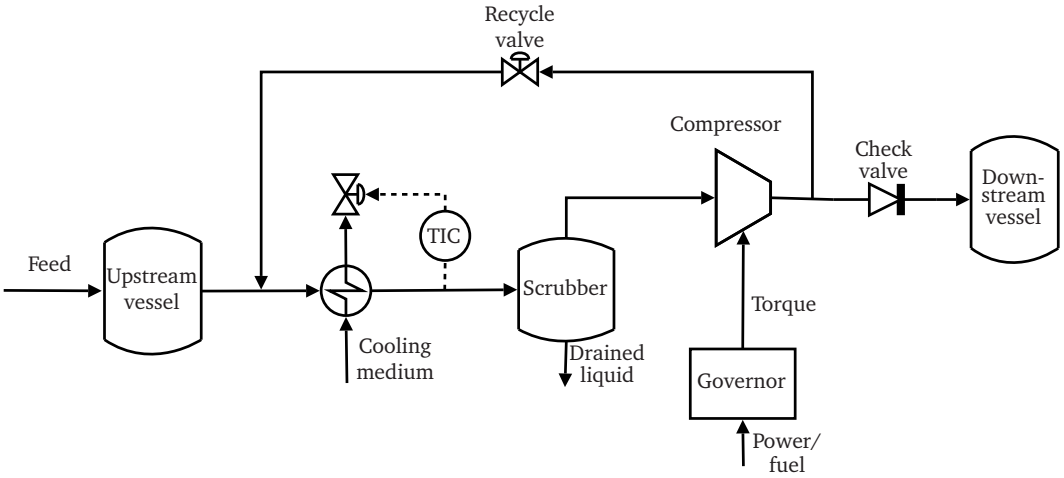

Figure 2.1: Diagram of the compressor system.

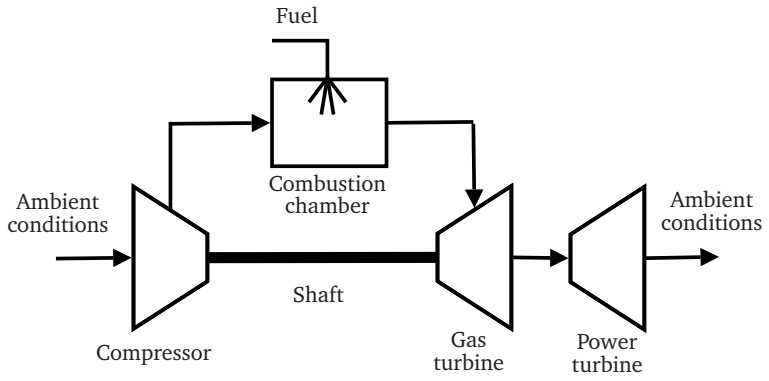

Figure 2.2: Diagram of the gas turbine system.

prevents the compressor from going into surge. The compressor governor is driven either with an electrical drive or by a gas turbine.

2.1.2 Gas turbine system

Gas turbines give a favourable power to weight ratio and are therefore popular drives on offshore installations. A typical gas turbine system consists of a compressor, which will be called the internal compressor to distinguish from the compressor in the compressor system, a combustor and one or two gas turbines. Air is compressed in the internal compressor and lead into the combustor. Heat is added to the gas by burning natural gas or other fuel in the combustor. The gas is further expanded over one or two gas turbines that drive the internal compressor and external loads.

Systems with one turbine are called single shaft systems. In these systems, the gas turbine drives both the internal compressor and an external load. The internal compressor and the gas turbine share a common shaft. A typical two shaft gas turbine system is shown in Figure 2.2. As for the single shaft system, the compressor is driven by the first turbine through a common shaft. However, this system has an extra gas turbine that is driven by the exhaust gas from the first gas turbine. Loads that are driven by the system are only connected to the second turbine.

The gas turbine systems on offshore installations can either be used to drive a power generator, which supplies the platform with electricity, or they can be used to drive equipment like compressors directly.

2.2 System components

2.2.1 Upstream vessel

The upstream vessel represents the upstream process and is the source of processing gas for the system. The upstream vessel can be modelled as a large closed volume fed with a mass flow that represents the mass flow from the upstream process. When mass flow out of the vessel is lower than the mass flow into the vessel, the pressure will increase, and vice versa. The vessel volume is large such that the vessel dynamics are slow relative to the compressor, scrubber and cooler dynamics. A sudden change in the mass flow in or out of the vessel will give a gradual change in pressure.

2.2.2 Downstream vessel

The downstream vessel represents the entire downstream process. In some cases, the downstream process is large enough to assume that the behaviour of compressor system does not affect the downstream process at all.

2.2.3 Cooler

A cooler is a device designed for heat transfer between two fluids. In this system the cooler is used for heat transfer between the processing gas and a cool-

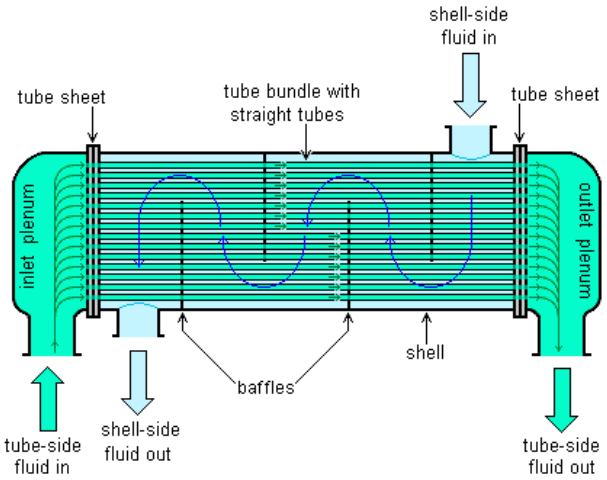

Figure 2.3: Straight-tube heat exchanger.

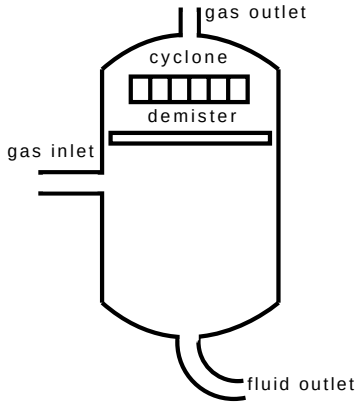

Figure 2.4: Scrubber illustration.

ing medium. Figure 2.3 shows a typical cooler where the processing gas flows through the tubes, which are surrounded with cooling medium. The shell side refers to the cooling medium side, and the tube side to the processing gas side since the tubes with the processing gas is surrounded by the cooling medium. There is continuous flow on both the shell and the tube side. The heat transfer rate depends on temperature difference between the fluids, flow rate through cooler, heat capacity of fluids and cooler design. A large surface area between the fluids will give better heat transfer, but it will also give more friction. The friction causes loss of pressure over the cooler.

2.2.4 Scrubber

The purpose of the scrubber is to remove the liquid, which is liquefied during the cooling stage, such that only saturated gas enters the compressor. The scrubber is a cylindrical vessel with inlet on the side, gas outlet on the top and fluid draining in the bottom, as shown in Figure 2.4. Inside the scrubber there is a rotating gas flow that will force the gas towards the scrubber wall. The heaviest droplets will hit the wall and flow to the bottom. The demister is usually some kind of mesh that catches more droplets. Finally, centripetal acceleration is used in the cyclone to remove the remaining droplets before the gas exits through the top outlet.

2.2.5 Centrifugal compressor

Compressors can be divided into two main categories, compressors that work by the principle of reducing the volume of the gas and continuous flow com-

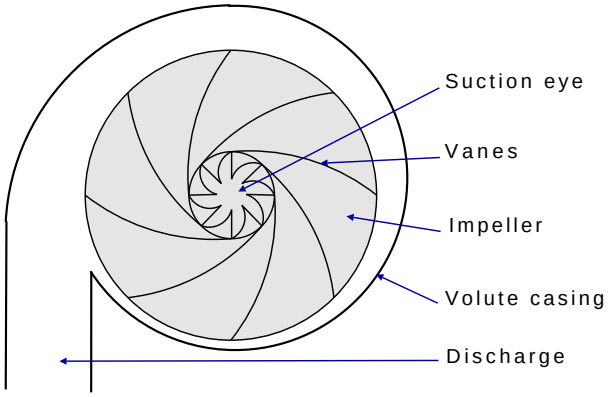

Figure 2.5: Compressor illustration.

pressors. The compressor modelled in this thesis is a centrifugal compressor, which is a continuous flow compressor. Figure 2.5 shows a basic sketch of a centrifugal compressor. The gas enters the compressor perpendicular to the impeller in the suction eye. Further, the gas is accelerated by the vanes on the rotating impeller and thrown toward the volute casing where the gas is decelerated and the kinetic energy is converted into potential energy. The conversion from kinetic to potential energy can be explained from Bernoulli's equation

$$\frac{p_1}{\rho_1} + \frac{C_1^2}{2} + gz_1 = \frac{p_2}{\rho_2} + \frac{C_2^2}{2} + gz_2,$$

where for $i \in \{1, 2\}$ the variables p_i, ρ_i, C_i and gz_i represents pressure, density, fluid velocity and potential energy, respectively. The rise in potential energy in a compressor is manifested in pressure rise. The subscripts 1 and 2 denote properties before and after deceleration. Bernoulli's equation is the law of conservation of energy for flowing fluids and says that the sum of kinetic energy $\frac{C_i^2}{2}$, potential energy gz_i and pressure head $\frac{p_i}{\rho_i}$ is constant from one set of conditions to another (Gravdahl and Egeland, 1998, p. 2-3).

2.2.6 Check valve

The check valve separates the compressor outlet from the downstream process. It is designed to prevent reversed flow and Figure 2.6 shows the principle of a check valve. When gas is flowing from the compressor to the downstream process, the check valve is open and the pressure drop is close to zero. The valve closes when the flow is reversed.

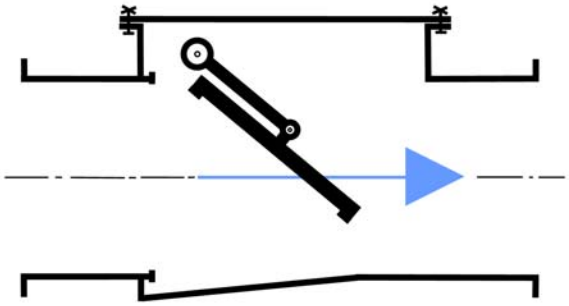

Figure 2.6: Check valve illustration.

2.2.7 Control valve

Control valves are used when there is a need for controlling the flow rate between to points. The control signal controls the valve stroke and for a certain valve the relation between valve stroke and flow is described by its characteristics. There will also be dynamics in the valve stroke. In this system control valves are used to control the compressor recycle flow and the cooler cooling medium flow.

2.2.8 Gas turbine

A gas turbine is used to convert potential energy from gas to kinetic energy. For an ideal gas turbine the gas is expanded adiabatic and all potential energy is converted into kinetic energy. For a real gas turbine the expansion is polytropic, hence some of the energy is transferred into heat that results in increased gas temperature. High pressure and high temperature gas is lead into the gas turbine where the pressure is lower on the outlet, and the gas drives a propeller like turbine wheel that is connected to a load.

2.2.9 Common shaft

The compressor is actuated by a gas turbine or an electric drive through a common shaft. The shaft connects the compressor impeller and the governor. As the system is running the shaft will rotate, and the drive will apply a torque in the rotational direction while the compressor will apply a torque in the opposite

direction.

In the gas turbine system there will be an internal compressor supplying air for the combustor and this compressor will also have a common shaft with the first gas turbine.

2.3 Ideal gas model

Ideal gas model says

$$pV = mRT, \tag{2.1}$$

where the notations are in accordance with the nomenclature. The gas constant R is given by

$$R = \frac{\bar{R}}{M},$$

where $\bar{R} = 8.314$ is the universal gas constant and M is the mole weight for the specific gas. In this system the compressor is compressing natural gas[1]. The mole weight for natural gas can vary between different wells and areas.

The ideal gas model is most accurate for gases at high temperatures and low pressures. The deviation from ideal gas can be quantified by a compressibility factor z defined by

$$z = \frac{pV}{mRT},$$

where $z = 1$ for ideal gas. Figure 2.7 shows the compressibility factor z as function of reduced pressure, p_r, and reduced temperature, T_r,

$$p_r = \frac{p}{p_c}, \quad T_r = \frac{T}{T_c},$$

where p_c is critical pressure and T_c is critical temperature. Reduced pressure and temperature are normalized values relative to the critical values. Experiments show that most gases have similar behaviour for the reduced pressure and temperature (Skogestad, 2000, p. 273-274).

For methane, which have properties similar to natural gas, the critical values are $p_c = 46bar$ and $T_c = 190K$ (*Air Liquide Encyclopaedia*, 2009). The process modelled in this thesis operates with gas in the pressure range $30 - 80bar$

[1]Natural gas is a mixture of hydrocarbon gases. It occurs with petroleum deposits, and is principally methane.

$\mathbf{p_r}$ \ $\mathbf{T_r}$	**1.58**	**2.21**
0.65	0.95	1.0
1.74	0.88	0.98

Table 2.1: Generalized compressibility diagram.

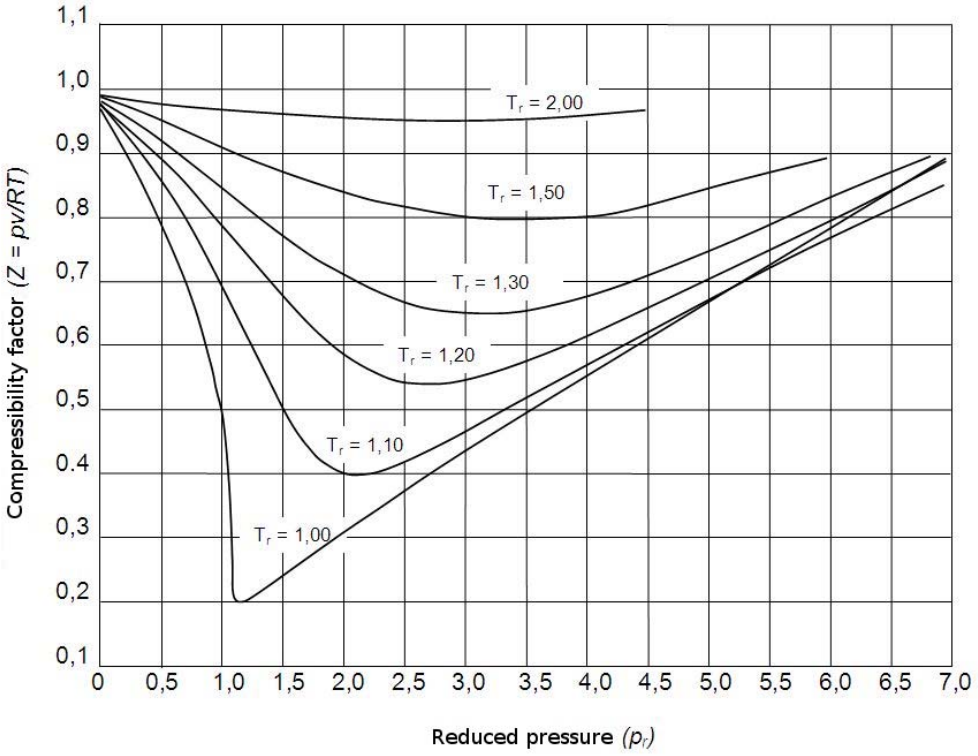

Figure 2.7: Generalized compressibilitydiagram.

and temperature $300 - 420K$. The reduced pressure and temperature will then be $p_r = [0.65 - 1.74]$ and $T_r = [1.58 - 2.21]$ respectively. Table 2.1 shows the compressibility factor z for some combinations of reduced pressure and temperature, and the worst case will give $z = 0.88$. Assuming ideal gas for the entire process will clearly give some deviations, but they will probably not change the behaviour of the system significant.

2.4 Internal energy, enthalpy and specific heats for ideal gas

The total energy E of a system can be divided into three components; kinetic energy, gravitational kinetic energy and other forms of energy. The other forms of energy is what we call internal energy U. Enthalpy H is a term closely related to internal energy and appears frequently in thermodynamic analysis. The relation between internal energy and enthalpy is

$$H = U + pV.$$

The specific heats c_v and c_p are defined

$$c_v = \frac{\partial u}{\partial T}\bigg)_v$$
$$c_p = \frac{\partial h}{\partial T}\bigg)_p,$$

where the subscript denotes the variable held fixed during differentiation. Note that U and H is the system internal energy and enthalpy, while u and h is specific internal energy and specific enthalpy such that $U = mu$ and $H = mh$.

For ideal gas the specific internal energy and enthalpy depends only on temperature such that

$$du = c_v(T)\, dT$$
$$dh = c_p(T)\, dT.$$

From ideal gas model (2.1) we also get

$$c_p(T) = c_v(T) + R.$$

Function for $c_p(T)$ have been approximated using fourth degree polynomials in Moran and Shapiro (2000, p. 838). Specific heats for air and methane at 300K and 1000K is shown in Table 2.2. Methane is chosen since it has similar properties to natural gas. For air the specific heat increases with 13% between 300K and 1000K, while for methane it increases with 102%. In further modelling, modules with large variations in temperature should allow for variations in specific heat.

2.5 Reynolds transport theorem

For fluid motion analysis we can either seek to describe the detailed flow pattern at every point, or work with a defined finite region, making balance of

Gas / T[K]	Air	Methane
300	1.005	2.221
1000	1.142	4.4758

Table 2.2: Specific heat air and methane for chosen values $[\frac{kJ}{kgK}]$.

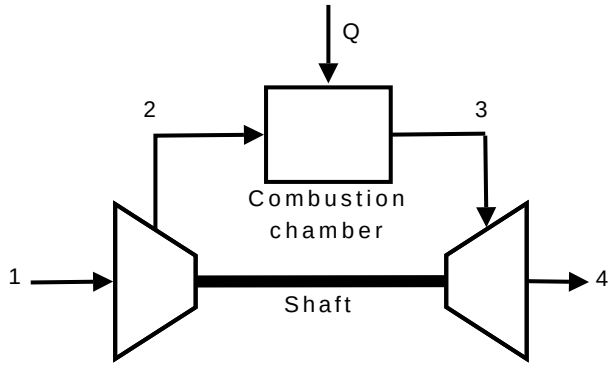

Figure 2.8: Simple gas turbine.

flow in versus flow out. The last approach leads to *Reynolds transport theorem* and control volume analysis. We are not interested in flow pattern or pressure and temperature distribution within a module, but the pressure, flow and temperature at the boundaries. This makes control volume analysis well suited for this purpose. Let us first define a control volume (CV), control surface (CS) and system (syst), which are subscripts used in the balance equations.

A CV is a volume defined for analysis, and the surface of the CV is called CS. The laws of mechanics are written for a system, which is an arbitrary quantity of mass. The law of physics states what happens when the system interacts with its surroundings. The CV can be fixed, moving and/or deforming. More details about *Reynolds transport theorem* are available in White (1999, p. 129-174). Equations for mass, momentum and energy balance are presented in Appendix B.

2.6 The Brayton cycle

A simple gas turbine is shown in Figure 2.8, and Figure 2.9 shows p-V- and T-s-diagram for an ideal Brayton cycle. In the p-V-diagram, the x-axis represents volume and the y-axis pressure. In the T-s-diagram, the x-axis represents en-

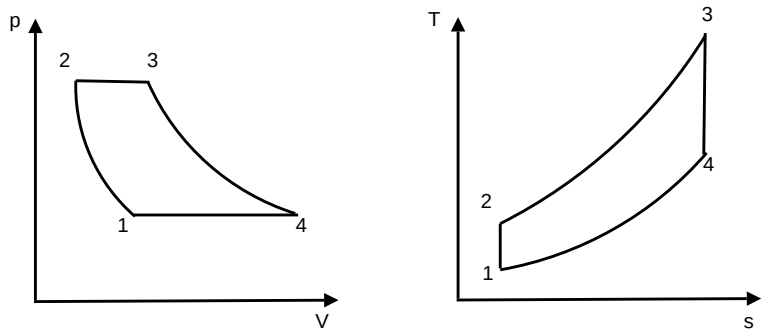

Figure 2.9: Ideal Brayton cycle.

tropy[2] and the y-axis temperature. Ambient air is compressed isentropic in step 1-2 as shown in Figure 2.8 and 2.9. In step 2-3 heat is added through isobaric combustion before the gas is expanded isentropic over a gas turbine in step 3-4. Finally the gas is cooled isobaric in step 4-1. For the system we are analyzing, step 1 fetches air from the environment, while the exhaust in 4 is released into the environment. No external cooler is needed.

2.7 Pipe friction

Gas flow in a pipe will always have some friction that can be related to loss of pressure. The pipe head loss h_f is in White (1999, p. 338-340) defined as

$$h_f = f\frac{L}{d}\frac{C^2}{2g},$$

where f is the Darcy friction factor, L the duct length, d the duct diameter, C the flow velocity and g the gravity constant. The pipe head loss can be related to pressure loss through

$$h_f = \frac{\Delta p}{\rho g},$$

such that

$$\Delta p = f\frac{\rho L C^2}{2d}.$$

The Darcy friction factor can be found in a Moody chart (White, 1999, p. 349). To use the Moody chart, the fluid Reynolds number must me known and is defined

$$Re = \frac{Cd}{\nu},$$

[2]Entropy is a quantitative measure for the amount of thermal energy not available to do work.

where ν is the fluid dynamic viscosity.

For compressor upstream conditions we want to find $\frac{\Delta p}{L}$ that denotes loss of pressure due to friction per meter. In White (1999, p. 770) the dynamic viscosity of air at $25°C$ is given $\nu = 1.5 \cdot 10^{-5}$, which we assume is close to the value of natural gas. The volume flow through the pipe when operating close to the compressor design point is approximately $q = 2300\frac{m^3}{h}$. For pipe diameter of $d = 0.3m$ the fluid velocity is $C = 9.0\frac{m}{s}$. The Reynolds number is then $Re = 1.80 \cdot 10^5$. Using the Moody chart in Figure 2.10 for stainless steel, which has relative roughness 0.002, gives the Darcy friction factor $f = 0.027$. The fluid density is from ideal gas model $\rho = \frac{p}{RT}$ which for $p = 32bar$, $R = \frac{8.314}{0.022}$ and $T = 298K$ gives $\rho = 28.4$. Inserting the values into (2.7) finally gives $\frac{\Delta p}{L} = 104$. For a 100m pipe, the friction loss would be $\Delta p = 1.04 \cdot 10^5 Pa = 0.104Bar$, which is very small to compared to the absolute pressure.

The values used in the approximations above are all gained from Section 4 and represent realistic process values.

2.8 Higher and lower heating value

The heating value of a fuel is the heat released by combusting a specific quantity of the fuel. The higher heating value (HHV) is the heat released by combustion when all water formed by the combustion is liquid, while the lower heating value (LHV) is obtained when all the water formed by the combustion is vapour (White, 1999, p. 716). The values are determined experimentally by combusting a specific amount of the given fuel at $25°C$. For the higher heating value, the product of the combustion is cooled back to $25°C$ and the released heat is used to calculate the HHV. For the lower heating value the product is cooler back to $150°C$, and the released heat is used to find LHV. More details about higher and lower heating values are available in Bossel (2003). Higher heating value will be used in this thesis since it represents all the heat released by combustion, including vaporizing water formed in combustion.

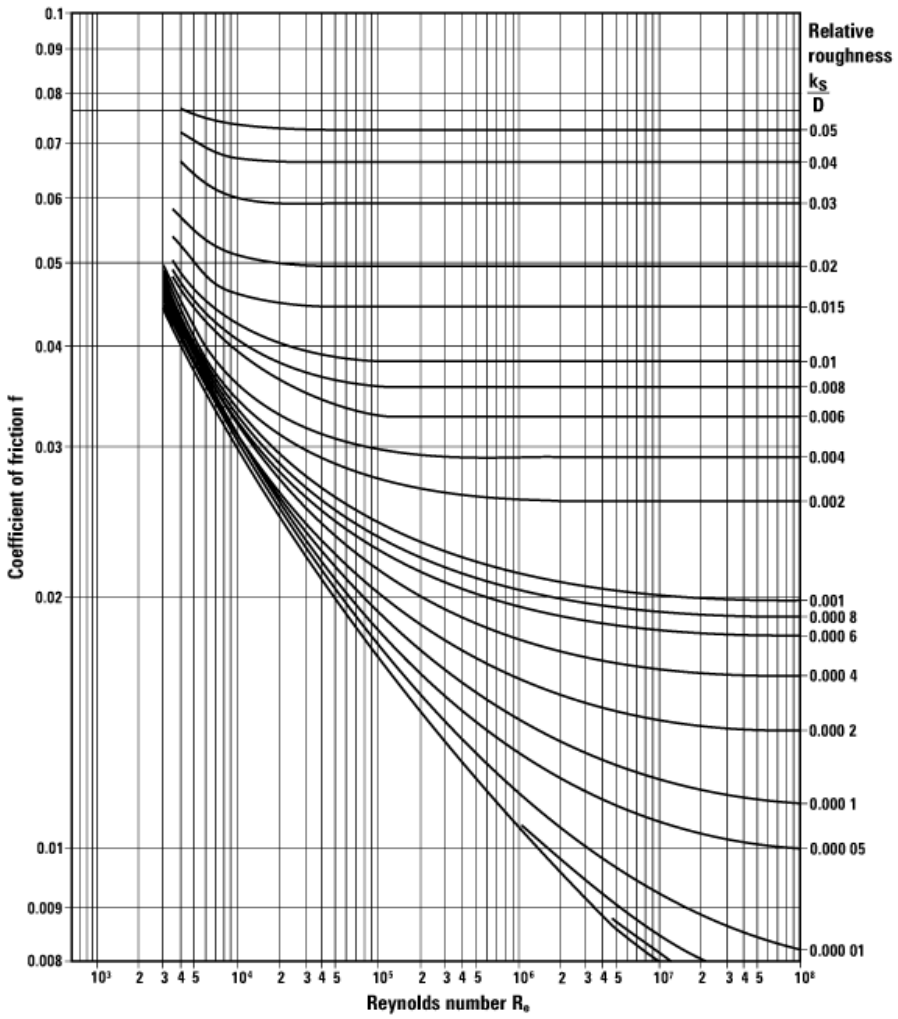

Figure 2.10: Moody chart (*Spirax Sarco, Pipes and pipe sizing*, 2009).

3 Modelling

In this section mathematical model of the compressor system is derived. Each element in the model is made as a module that can be connected in a network description (Egeland and Gravdahl, 2002, p. 19-20). The different modules are connected with arrows showing the direction of the signal flow. Input and output refers to signals, while inlet and outlet refers to the process. For example, the compressor inlet is where the gas enters the compressor, while a compressor input represents a signal entering the compressor and can be related to the compressor outlet conditions. The modules will be implemented and connected in Simulink®. The system dynamics are described with differential equations.

When making the system based on modules it can easily be upgraded by simply upgrading the respective modules. The system layout can also be changed and extended by rearranging, removing or adding modules. The modules can easily be tested one by one before adding them to the network.

Each module is modelled with general subscripts where in and out represents an inlet and an outlet respectively, while no subscript represents a state. Constants are allocated subscripts after the same convention.

Figure 3.1 shows the compressor system modules and their interconnections. In this figure the variables are assigned subscripts described in Appendix E. The process modules can be divided into three categories:

- Modules with pressure dynamics, called pressure modules.
- Modules with flow dynamics, called flow modules.
- Modules with neither pressure nor flow dynamics, called static modules.

In addition to the process modules there is a mechanical module, the shaft, that represents the connection between compressor and governor.

For a pressure module, pressure is defined as a module state and the pressure differential equation depends on the inlet and the outlet flows. The vessel is an example of a pressure module. Flow modules have flow defined as a module state, and the flow differential equation depends on the inlet and the outlet pressures. The duct module fits into this category. Two pressure modules can not be placed next to each other, but have to be separated by a flow module. Similarly can not two flow modules be placed next to each other, but have to be separated by a pressure dynamics module. In addition, the pressure and the flow modules can yet again be separated by the static modules. The static modules can have temperature dynamics, like the cooler, but some are also without dynamics like the manifold and the split.

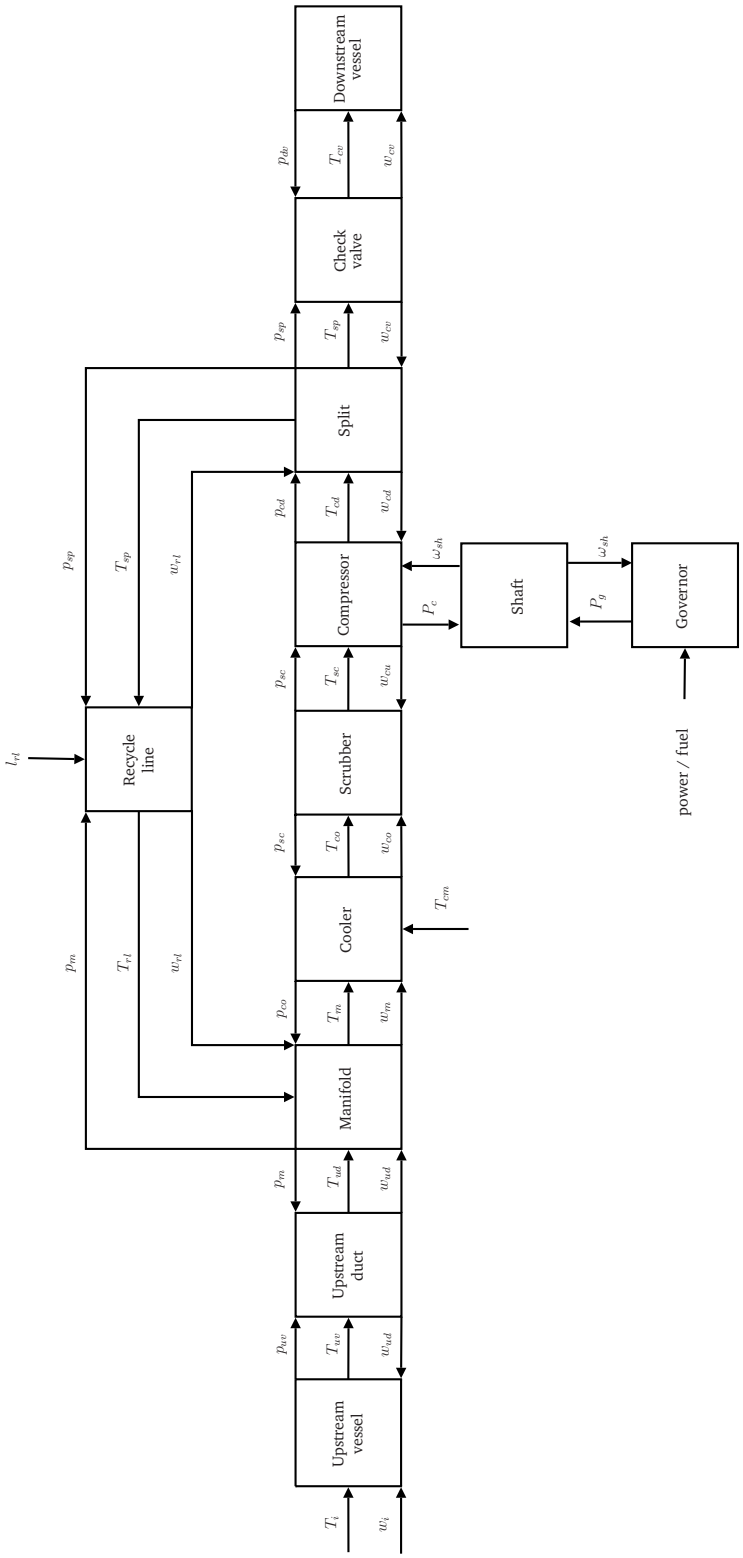

Figure 3.1: Compressor system modules.

The pressure modules are derived using the mass balance equation (B.1), and flow modules are derived using the momentum balance equation (B.2). For modules that in addition have temperature dynamics, the energy balance equation (B.3) is used.

The first module in Figure 3.1 is the upstream vessel, which is a pressure module, followed by the upstream duct flow module. The two next modules, manifold and cooler, are static modules, and connects the upstream duct with the scrubber pressure module. Similarly is the recycle line flow module connected with the scrubber pressure module through the manifold and cooler static modules. The compressor module is an exception from our rule since it actually is a flow and a pressure module interconnected. The recycle line and the check valve, which both are flow modules, are connected to the compressor outlet volume. Finally the check valve is connected to the downstream vessel pressure module where the volume is modelled infinitely large such that the pressure is constant. The shaft connects the compressor and the governor with a momentum equation.

Figure 3.2 shows the gas turbine with similar representation. The compressor and the turbines are flow modules in this system, and they are separated by a combustor volume and a volume between the turbines, which both are pressure modules. The compressor downstream volume is in this model represented as a part of the combustor volume.

When modelling modules for a large model it is important to keep in mind the purpose of the model. The model is designed for anti-surge control validation. The main focus should therefore be to:

1. Make an accurate model of the compressor pressure, flow and temperature at both inlet and outlet for steady state and transients.

2. Make an sufficiently accurate model of the process around the compressor.

3. Model the compressor and governor speed dynamics.

Some elements in the compressor system will represent fast dynamics and other slower. Before making an effort of modelling fast dynamics one should keep in mind how much this dynamics will affect the compressor behaviour and surge limit. Perhaps the fast dynamics will be damped out by elements with slower dynamics.

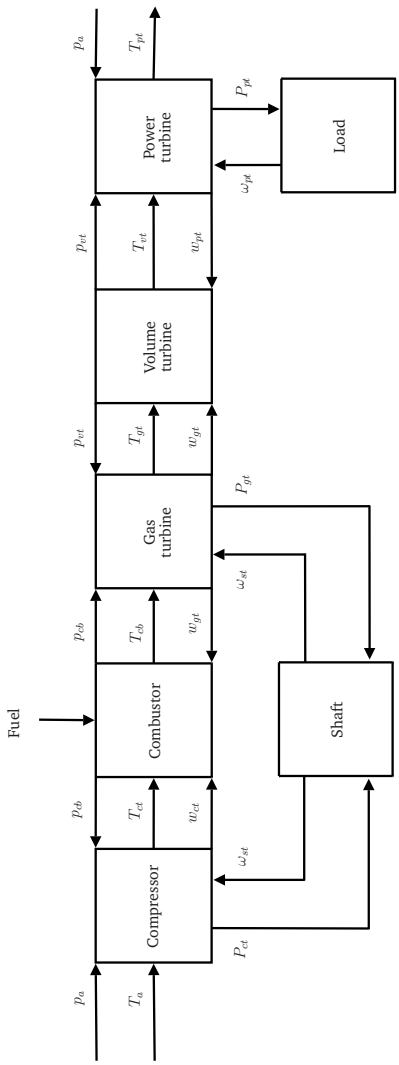

Figure 3.2: Turbine system modules.

3.1 Duct

The duct module represents piping in the system and its flow dynamics can be modelled using the momentum balance from (B.2). Assuming no mass accumulation in the duct and uniform mass flow over the entire length gives

$$\frac{\mathrm{d}}{dt}\left(\int_{CV}\rho\vec{C}\,dV\right)=\frac{\mathrm{d}}{dt}(\rho A\vec{C})\int_{L}dL=\frac{\mathrm{d}w}{dt}L,$$

where CV refers to the control volume we are analysing. More details about CV analysis is available in Appendix B. Further assuming one-dimensional flow

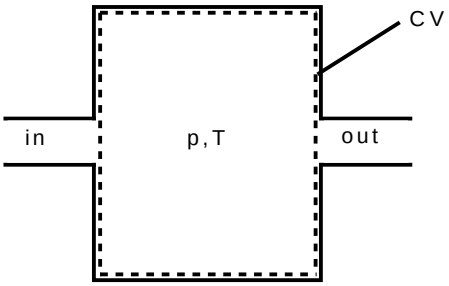

Figure 3.3: Vessel control volume.

as stated in Appendix B and incompressible flow, the momentum flux becomes

$$\sum_i (\dot{m}_i \vec{C}_i)_{out} - \sum_i (\dot{m}_i \vec{C}_i)_{in} = 0.$$

Forces acting on this system is the surface pressures at the inlet and the outlet, and forces F generated by friction or equipment between the inlet and the outlet like a compressor or a valve. The resulting flow dynamics is

$$L\dot{w} = A_{in}p_{in} - A_{out}p_{out} + F, \tag{3.1}$$

where $F > 0$ for components adding energy to the duct, while $F < 0$ for components or phenomena absorbing energy from the duct.

Heat loss in the duct is considered small and is neglected. Temperature can be analysed using partial differential equation. However, we are interested in one dimensional transient behaviour. For slow variations in the inlet temperature and high fluid velocity C we can assume $T_{in} = T_{out}$.

The duct module will have three signal inputs, p_{in}, p_{out} and T_{in}, and two outputs, T_{out} and w.

3.2 Vessel

A vessel will be used to model the upstream and the downstream vessel, and the scrubber. It can also be used as a modelling element to represent pressure dynamics somewhere, like at the compressor outlet. The vessel is analysed using a fixed control volume, and mass and energy balance. Using (B.1) gives

$$\frac{\mathrm{d}m}{dt} = w_{in} - w_{out}. \tag{3.2}$$

The energy balance is given by (B.3). We assume the volume is large and thermal energy dominates kinetic energy such that the velocity C inside the volume can be neglected. We also assume uniform temperature and pressure over

the entire volume, and that the potential energy due to gravitation can be neglected. By removing the terms from (B.3) corresponding to our assumptions the resulting equation is

$$\dot{Q} - \dot{W} = \frac{\mathrm{d}}{dt}\left(\int_{CV} u\rho\, dV\right) + \sum h_{out}\dot{m}_{out} - \sum h_{in}\dot{m}_{in},$$

where h_{out} relates to specific enthalpy inside the control volume, $\dot{m}_{out} = w_{out}$ and $\dot{m}_{in} = w_{in}$. Rearranging the equation and solving the CV integral gives

$$\frac{\mathrm{d}}{dt}(mu) = h_{in}w_{in} - hw_{out} + \dot{Q} - \dot{W},$$

where the specific internal energy u can be related to temperature such that $u = c_v T$, and equivalent with specific enthalpy $h = c_p T$. Inserting into equation above gives

$$\begin{aligned}\frac{\mathrm{d}}{dt}(mc_vT) &= c_pT_{in}w_{in} - c_pTw_{out} + \dot{Q} - \dot{W}\\ \frac{\mathrm{d}m}{dt}c_vT + mc_v\dot{T} &= c_pT_{in}w_{in} - c_pTw_{out} + \dot{Q} - \dot{W},\end{aligned} \tag{3.3}$$

where $\frac{\mathrm{d}m}{dt}$ is given from the mass balance. Inserting (3.2) into (3.3) gives

$$(w_{in} - w_{out})c_vT + mc_v\dot{T} = c_pT_{in}w_{in} - c_pTw_{out} + \dot{Q} - \dot{W} \tag{3.4}$$

Rearranging (3.4) and inserting from ideal gas model (2.1) gives

$$\begin{aligned}\dot{T} &= \frac{RT}{pVc_v}\left[c_pT_{in}w_{in} - \left((c_p - c_v)w_{out} + c_vw_{in}\right)T + \dot{Q} - \dot{W}\right]\\ &= \frac{RT}{pV}\left[\kappa T_{in}w_{in} - \left((\kappa-1)w_{out} + w_{in}\right)T + \frac{1}{c_v}(\dot{Q} - \dot{W})\right],\end{aligned} \tag{3.5}$$

which is the temperature dynamics of a closed vessel that will be used in the model.

To obtain the pressure dynamics, the ideal gas model (2.1) is used to rearrange the energy balance equation hence

$$mu = mc_vT = \frac{1}{R}c_vpV.$$

The energy balance for this case becomes

$$\frac{\mathrm{d}}{dt}\left(\frac{1}{R}c_vpV\right) = h_{in}w_{in} - hw_{out} + \dot{Q} - \dot{W}. \tag{3.6}$$

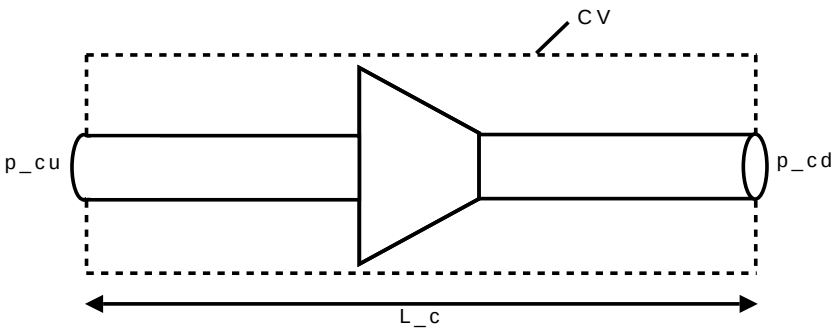

Figure 3.4: Compressor control volume for momentun balance.

Inserting for specific enthalpy into (3.6) gives

$$\begin{aligned}\frac{1}{R}c_v\frac{\mathrm{d}p}{dt}V &= c_pT_{in}w_{in} - c_pTw_{out} + \dot{Q} - \dot{W} \\ &= c_pT_{in}w_{in} - c_pTw_{out} + \dot{Q} - \dot{W}.\end{aligned} \tag{3.7}$$

Rearranging (3.7) gives

$$\dot{p} = \frac{\kappa R}{V}\left(T_{in}w_{in} - Tw_{out} + \frac{1}{c_p}(\dot{Q} - \dot{W})\right), \tag{3.8}$$

which is the resulting pressure dynamics for the vessel.

For a closed vessel with inlet flow w_{in} with temperature T_{in} and outlet flow w_{out}, the temperature and pressure dynamics are given by (3.5) and (3.8). This gives a module with signal inputs w_{in}, w_{out} and T_{in} and signal outputs T and p.

3.3 Compressor

Figure 3.4 shows the compressor between to ducts surrounded by a control volume for analysis. We want to derive the flow dynamics equation based on momentum balance. Let the control volume include the ducts and the compressor. Let us further use the same assumptions as for the duct module; no mass accumulation in the duct and uniform mass flow over the entire length. The result from (3.1) gives:

$$L\dot{w} = A_{in}p_{in} - A_{out}p_{out} + F, \tag{3.9}$$

where F in this case will represent the force applied by the compressor.

Let Ψ represent the pressure ratio between inlet and outlet at steady state such that

$$\Psi = \frac{p_{out}}{p_{in}},$$

and at steady state $\dot{w} = 0$ hence

$$A_{in}p_{in} - A_{out}\Psi p_{in} + F = 0. \tag{3.10}$$

Finally inserting (3.10) into (3.9) gives

$$\begin{aligned} L\dot{w} &= A_{in}p_{in} - A_{out}p_{out} + A_{out}\Psi p_{in} - A_{in}p_{in} \\ &= A_{out}(\Psi p_{in} - p_{out}). \end{aligned} \tag{3.11}$$

The outlet pressure dynamics are modelled by adding a volume at the compressor outlet. A volume model can be found in Section 3.2 resulting in (3.5) and (3.2). However, this volume also includes temperature dynamics and will give unnecessary complex dynamics that can slow down the simulation without making the model noticeably better. Rapid variations in outlet temperature will be damped out during recycle, cooling and scrubbing and is therefore not essential for the overall behaviour. A simpler volume model will be used here.

If the volume of the downstream duct is relative small compared to the mass flow through the compressor, it is reasonable to assume that the temperature out of the volume is equal to the temperature out of the compressor. The volume temperature will then follow the temperature from the compressor outlet instead of (3.5). For the pressure dynamics, we have from (3.2)

$$\dot{p} = \frac{\kappa R}{V}\left(T_{in}w_{in} - Tw_{out} + \frac{1}{c_p}\dot{Q}\right),$$

where we now assume $T_{in} = T_{out} = T$ is the compressor downstream temperature, $w_{in} = w$ is mass flow from the duct into the volume and w_{out} is the mass flow out of the volume. The heat transfer with the environment, $\dot{Q}$, will further be neglected. The pressure dynamics is

$$\dot{p} = \frac{\kappa RT}{V}\left(w - w_{out}\right). \tag{3.12}$$

The compressor downstream temperature T_{out} is according to Venturini (2005) and Gravdahl (2001)

$$T_{out} = T_{in}\left(\frac{p_{out}}{p_{in}}\right)^{\frac{\kappa-1}{\kappa\eta}}, \tag{3.13}$$

for a polytropic process where η is the polytropic efficiency of the compressor, which can be found from experimental data. The polytropic equation is also given in (C.4).

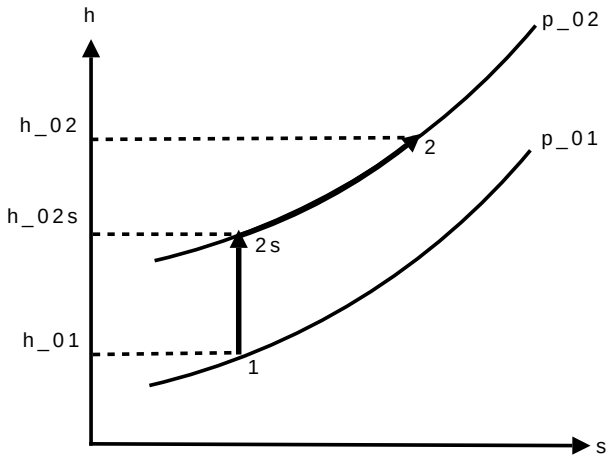

Figure 3.5: Compressor phase diagram.

The compressor pressure ratio chart is given as a function of volume flow and compressor speed, and we need a way to cast this function to fit the representation used in this model. Assume that $\Psi_q : \mathbb{R} \times \mathbb{R} \to \mathbb{R}$ represents the compressor pressure ratio curves such that

$$\Psi_q(q, N) = \frac{p_{out}}{p_{in}},$$

where q is volume flow through the compressor and N is compressor rotational speed in revolutions per minute. Let $\Psi_w : \mathbb{R} \times \mathbb{R} \to \mathbb{R}$ represent the same pressure ratio, but with mass flow and angular velocity as input arguments. Ideal gas model (2.1) gives

$$q = w\frac{zRT_{in}}{p_{in}},$$

and the mapping between revolutions per minute and angular velocity is

$$N = \omega\frac{30}{\pi},$$

then the relation between Ψ_q and Ψ_w is

$$\Psi_w(w, \omega) = \Psi_q(q, N)|_{q=w\frac{zRT_{in}}{p_{in}}, N=\omega\frac{30}{\pi}}.$$

Further, we want to find a compressor pressure ratio function that includes the inlet temperature T_{in} as input parameter in addition to the flow and speed. According to Egeland and Gravdahl (2002, p. 494), the compressor pressure

ratio $\Psi_T : \mathbb{R}^3 \to \mathbb{R}$ can be expressed as

$$\Psi_T(w, \omega, T_{in}) = \left(1 + \frac{\Delta h_{02s}(w, \omega)}{c_p T_{in}}\right)^{\frac{\kappa}{\kappa-1}}, \tag{3.14}$$

where $\Delta h_{02s}(w, \omega) = h_{02s} - h_{01}$ is the enthalpy rise shown in Figure 3.5. The enthalpy rise is split into an isentropic process h_{02s} due to the reversible work and an isobaric process h_{01} due to non-reversible work. We want to find h_{02s} represented with the known function Ψ_w. Rearranging (3.14) gives

$$\Delta h_{02s} = c_p T_{in} \left(\Psi_T(w, \omega, T_{in})^{\frac{\kappa-1}{\kappa}} - 1\right). \tag{3.15}$$

The experimental compressor chart in Figure 3.6 is given for a specific temperature T_0 such that

$$\Psi_T(w, \omega, T_{in})|_{T_{in}=T_0} = \Psi_w(w, \omega), \tag{3.16}$$

and from (3.15) and (3.16) one get

$$\Delta h_{02s} = c_p T_0 \left(\Psi_w(w, \omega)^{\frac{\kappa-1}{\kappa}} - 1\right), \tag{3.17}$$

which is the enthalpy rise represented with the known function $\Psi_w(w, \omega)$. Inserting (3.17) back into (3.14) gives

$$\begin{aligned} \Psi_T(w, \omega, T_{in}) &= \left(1 + \frac{c_p T_0 \left(\Psi_w(w, \omega)^{\frac{\kappa-1}{\kappa}} - 1\right)}{c_p T}\right)^{\frac{\kappa}{\kappa-1}} \\ &= \left(1 + \frac{T_0}{T}\left(\Psi_w(w, \omega)^{\frac{\kappa-1}{\kappa}} - 1\right)\right)^{\frac{\kappa}{\kappa-1}} \\ &= \left(\left(1 - \frac{T_0}{T}\right) + \frac{T_0}{T}\Psi_w(w, \omega)^{\frac{\kappa-1}{\kappa}}\right)^{\frac{\kappa}{\kappa-1}}, \end{aligned} \tag{3.18}$$

which expresses the compressor pressure ratio as a function of flow, speed and temperature.

3.3.1 Pressure ratio chart

The compressor pressure ratio Ψ_q is based on experimental values. Figure 3.6 shows a compressor chart where the different curves represents different compressor shaft speed, the x-axis represents volume flow through the compressor and the y-axis the pressure ratio between inlet and outlet. An approximation of

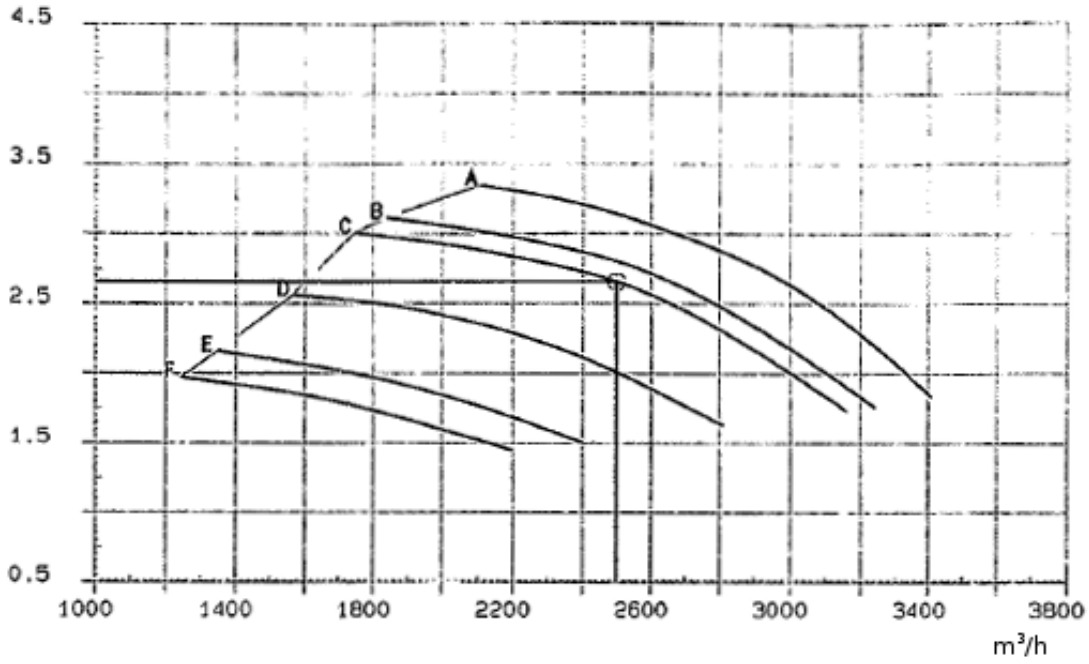

Figure 3.6: Compressor pressure ratio chart.

the compressor curve $\Psi_q(q, N)$ is derived by utilizing curve fitting in the sense that

$$\Psi_q(q, N) = c_1(N)q^3 + c_2(N)q^2 + c_3(N)q + c_4(N), \tag{3.19}$$

where each $c_i : \mathbb{R} \to \mathbb{R}, i \in \{1, 2, 3, 4\}$ is calculated by yet another polynomial approximation:

$$c_i(N) = c_{i1}N^3 + c_{i2}N^3 + c_{i3}N + c_{i4}. \tag{3.20}$$

The polynomial orders can be reduced if it turns out that lower order gives sufficient accurate approximation.

3.3.2 Polytropic efficiency chart

Figure 3.7 shows the compressor polytropic efficiency as a function of volume flow through the compressor and compressor shaft speed. Let $\Phi_q : \mathbb{R} \times \mathbb{R} \to \mathbb{R}$ define a mapping of the polytropic efficiency such that

$$\Phi_q(q, N) = \eta. \tag{3.21}$$

An approximation of the efficiency curve Φ_q is also derived utilizing curve fitting on Figure 3.7 such that

$$\Phi_q(q, N) = d_1(N)q^3 + d_2(N)q^2 + d_3(N)q + d_4(N), \tag{3.22}$$

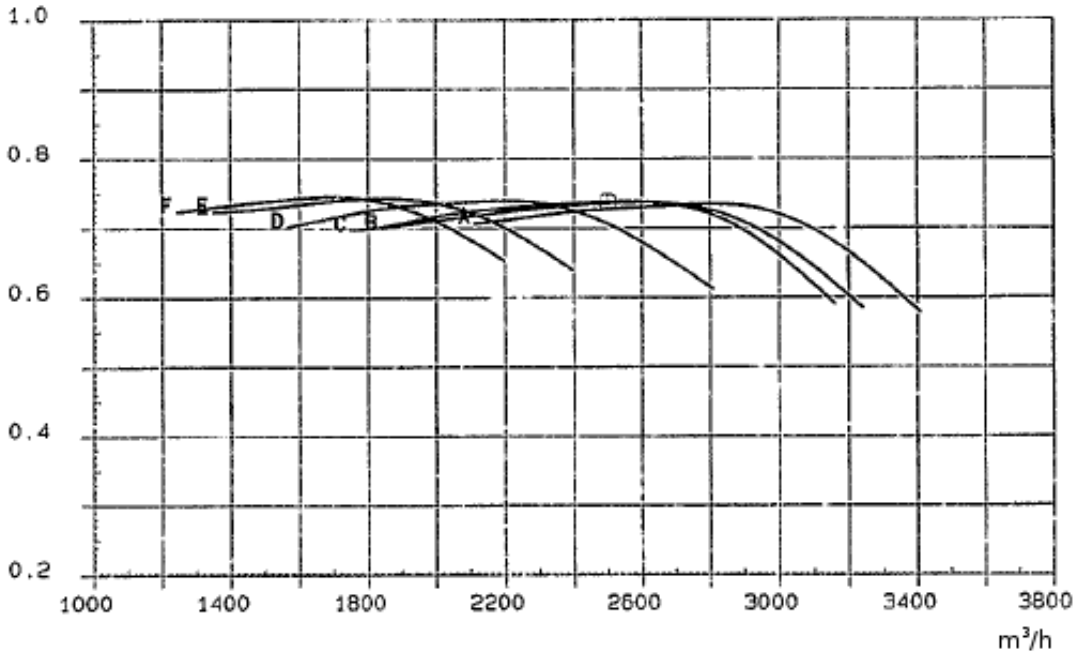

Figure 3.7: Compressor polytropic efficency chart.

where each $d_j : \mathbb{R} \to \mathbb{R}, j \in \{1, 2, 3, 4\}$ is calculated with polynomial approximation:

$$d_i(N) = d_{i1}N^3 + d_{i2}N^3 + d_{i3}N + d_{i4}. \tag{3.23}$$

3.3.3 Compressor drive torque

The compressor is driven by either an electrical motor or a gas turbine. The shaft dynamics are modelled in Section 3.14. According to Egeland and Gravdahl (2002, p. 488) the compressor torque τ_l is approximately

$$\tau_c = k_c w_c \omega,$$

where k_l is a friction constant.

Morini et al. (2007) suggest

$$\tau = \frac{w c_p T_{in}}{\omega} \left[\left(\frac{p_{out}}{p_{in}} \right)^{\frac{\kappa-1}{\kappa\eta}} - 1 \right] = \frac{w c_p T_{in}}{\omega} \left(\Psi^{\frac{\kappa-1}{\kappa\eta}} - 1 \right),$$

which is based on that the shaft power equals the energy added to the gas during a polytropic compression (C.4).

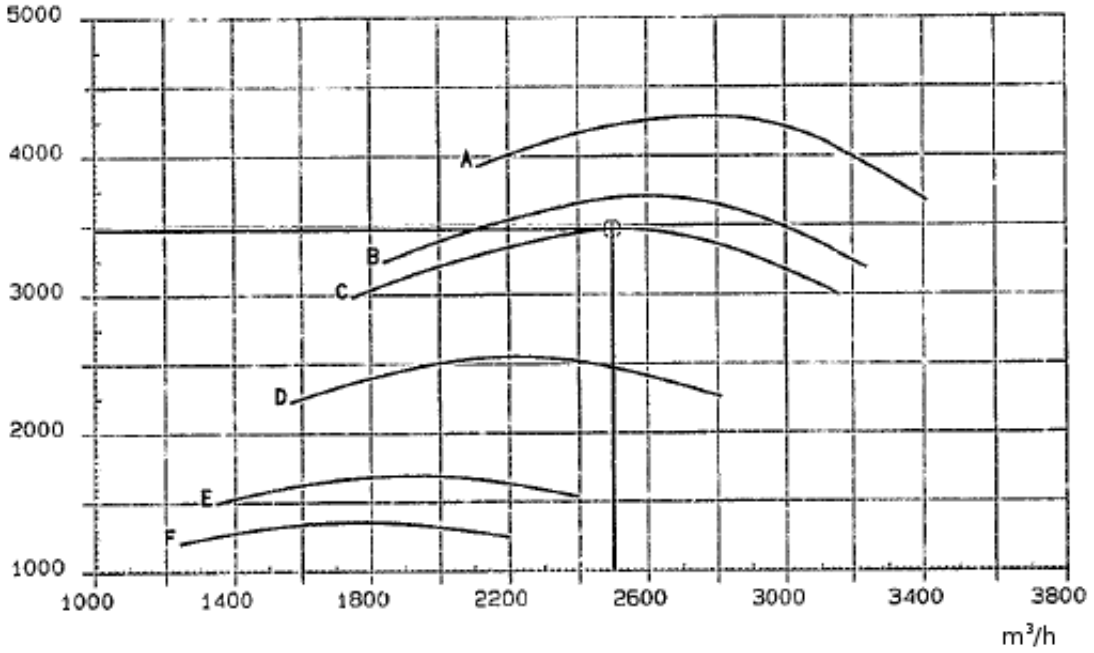

Figure 3.8: Compressor shaft power in kW.

The third approach is to use experimental data. Figure 3.8 shows compressor shaft power as a function of volume flow and speed. The x-axis represents volume flow $[\frac{m^3}{h}]$, the y-axis represents shaft power $[kW]$ and the curves denoted A-F represent different speed curves. Let $\Gamma_q : \mathbb{R} \times \mathbb{R} \rightarrow \mathbb{R}$ define a mapping of the compressor shaft power such that

$$\Gamma_q(q, N) = P,$$

which can be approximated using polynomial fit as for the compressor pressure ratio chart and efficiency chart. This approach is probably the most accurate when operating within the range the chart is defined for. However, in cases when a such chart is unavailable, for example in surge, other methods must be considered.

3.4 Manifold

The manifold is a mixing unit and a static module. It is used to merge the flow from the upstream vessel with the flow from the recycle line into the cooler. We assume no loss of pressure through the manifold.

Let the inlets be denoted with subscript $in, 1$ and $in, 2$. The module input parameters are mass flow and temperature at the inlet, and pressure at the outlet. The

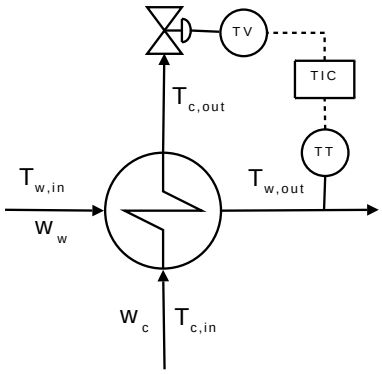

Figure 3.9: Cooler inputs and outputs.

module output parameters are flow and temperature at the outlet and pressure at the inlet.

The gas flow out of the manifold is the sum of the gas flows in, hence

$$w_{out} = w_{in,1} + w_{in,2}.$$

Since the manifold is a static module, there is no accumulation inside the module and energy into the manifold is equal the energy out. The pressure is equal at both sides and flow energy is neglected, hence

$$\dot{E}_{in,1} + \dot{E}_{in,2} = \dot{E}_{out},$$
$$w_{in,1}\, c_v(T_{in,1})\, T_{in,1} + w_{in,2}\, c_v(T_{in,2})\, T_{in,2} = w_{out}\, c_v(T_{out})\, T_{out}.$$

We assume the difference in temperature for the inlet flows is small such that we can assume that c_v is constant hence

$$T_{out} = \frac{1}{w_{in,1} + w_{in,2}} \left(w_{in,1} T_{in,1} + w_{in,2} T_{in,2}\right). \tag{3.24}$$

3.5 Cooler

The cooler is a counter flow heat exchanger. The pressure drop is assumed like zero for both processing gas and cooling medium, and the mass flow is uniform over the entire cooler both on warm and cold side.

Figure 3.9 shows the cooler with inputs, outputs and controller. Heat can be transferred between a warm and a cold side, where the heat transfer rate $\dot{Q}$ is given

$$\dot{Q} = UHA\Delta T, \tag{3.25}$$

where UH is a heat transfer coefficient, A is surface area between cold and warm side and ΔT is temperature difference between warm and cold side (Skogestad, 2000, p. 111).

Due to constant pressure during cooling, the gas will contract continuously over the entire cooler. Modelling this in detail requires that we study the partial derivatives over the entire length. Heat transfer will be affected of varying density of the gas as it contracts. However, we are only interested in the transient behaviour at the outlet.

Let us start with modelling heat exchange between two volumes, a cold and a warm, denoted with subscripts c and w respectively. The cold side is a liquid cooling medium, and the warm side is the processing gas we want to cool. Let $\dot{Q}_c$ denote the heat transfer to the cold side and $\dot{Q}_w$ to the warm side. We use the energy balance from (B.3), and assume that thermal energy dominates kinetic and potential energy. We also know that the work done by the cooler on the environment is zero. From the assumptions we get

$$\begin{aligned}\dot{Q} &= \frac{\mathrm{d}}{dt}\left[\int_{CV} \rho u \, dV\right] + h_{out}w_{out} - h_{in}w_{in} \\ &= \frac{\mathrm{d}}{dt}(mu) + h_{out}w_{out} - h_{in}w_{in}.\end{aligned} \tag{3.26}$$

The cooling medium is a liquid and incompressible. For incompressible fluids is the internal energy and the enthalpy equal (Moran and Shapiro, 2000, p. 109) hence $u = h = c_pT$. Inserted into (3.26) gives

$$\frac{\mathrm{d}}{dt}(m_c c_{p,c} T_c) = h_{c,in}w_{c,in} - h_c w_{c,out} + \dot{Q}_c,$$

and for the warm side $u = c_vT$ and $h = c_pT$ hence

$$\frac{\mathrm{d}}{dt}(m_w c_{v,w} T_w) = h_{w,in}w_{w,in} - h_c w_{w,out} + \dot{Q}_w.$$

The specific heat is a function of temperature but its derivative with respect to temperature is small and we assume the specific heats are constant. To reduce error, specific heat values are chosen as the mean value between specific heat at the inlet and the outlet. The heat transfer between warm and cold side is given by (3.25) such that $Q_c = -Q_w = UHA(T_w - T_c)$. Inserting for $\dot{Q}$ gives

$$\begin{aligned}m_w c_{v,w}\dot{T}_w &= c_{p,w}T_{w,in}w_{w,in} - c_{p,w}T_w w_{w,out} - UHA(T_w - T_c), \\ m_c c_{p,c}\dot{T}_c &= c_{p,c}T_{c,in}w_{c,in} - c_{p,c}T_c w_{c,out} + UHA(T_w - T_c).\end{aligned}$$

To approximate a counter flow heat exchanger, several control volumes can be interconnected in series as shown in Figure 3.10, where n represents the

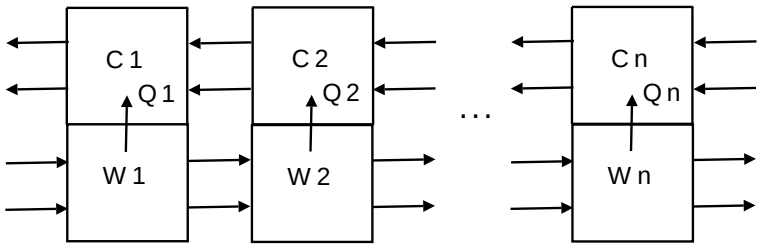

Figure 3.10: Heat exchanger volumes interconnected.

number of interconnected modules. A higher n value will give a more efficient heat exchanger. Interconnecting n modules will result in this system:

$$\begin{aligned}
\dot{T}_{ci} &= \frac{1}{m_c c_{p,c}} \left[-(\frac{UHA}{n} + c_{p,c} w_c) T_{ci} + c_{p,c} w_c T_{c(i+1)} + \frac{UHA}{n} T_{wi} \right] \\
&\qquad for\, i \in [1, n-1] \\
\dot{T}_{cn} &= \frac{1}{m_c c_{p,c}} \left[-(\frac{UHA}{n} + c_{p,c} w_c) T_{cn} + c_{p,c} w_c T_{c,in} + \frac{UHA}{n} T_{wn} \right] \\
\dot{T}_{w1} &= \frac{1}{m_w c_{v,w}} \left[-(\frac{UHA}{n} + c_{p,w} w_w) T_{w1} + c_{p,w} w_w T_{w,in} + \frac{UHA}{n} T_{c1} \right] \\
\dot{T}_{wi} &= \frac{1}{m_w c_{v,w}} \left[-(\frac{UHA}{n} + c_{p,w} w_w) T_{wi} + c_{p,w} w_w T_{w(i-1)} + \frac{UHA}{n} T_{ci} \right] \\
&\qquad for\, i \in [2, n].
\end{aligned} \tag{3.27}$$

3.5.1 Cooler controller

The cooler is controlled by a PI-controller that uses the outlet temperature on warm side as the signal input, and the cooling medium flow valve as the signal output such that

$$\begin{aligned}
u &= PI(e) \\
e &= y_{ref} - y,
\end{aligned}$$

where $PI(.)$ represent the PI-controller, while the valve stroke set point $l_{tv} = u$ and $T_{w,out} = y$.

The controller output u is saturated such that $u \in [0, 100]$. For a controller with integrator, the integrator will continue increasing even after the valve is saturated as described in Balchen et al. (2003, p. 534-536). To prevent this the PI-controller needs anti-windup and a possible structure is shown in Figure 3.11.

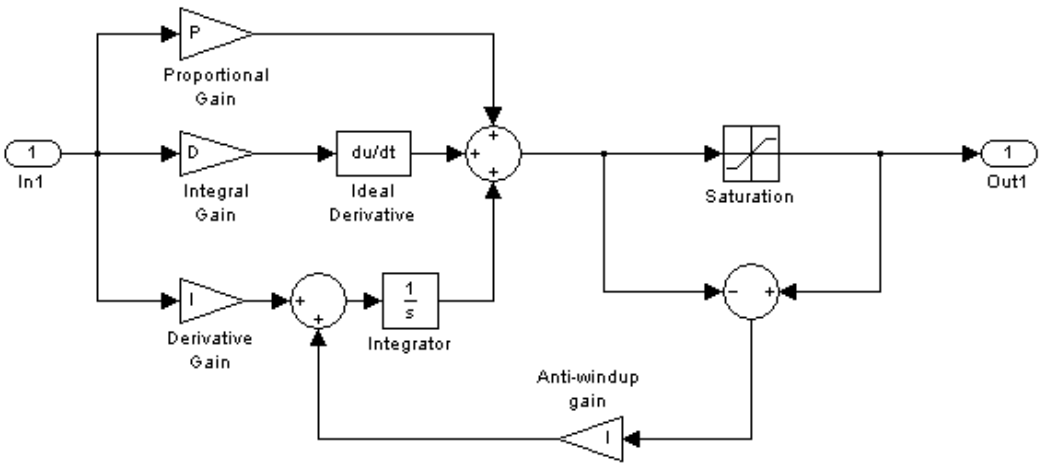

Figure 3.11: PI-controller with anti-windup.

3.6 Scrubber

The scrubber is a two phase flow component and the mass flow to the compressor is less than the mass flow into the scrubber since some liquid is drained. The drained liquid gas can be taken into the model by using phase diagram to calculate how much of the gas condensates. However, we will first make a simple one phase model and then consider extension if necessary.

The scrubber will be modelled as a vessel with no heat loss. Heat loss can later be introduced if necessary.

3.7 Check valve

The check valve will be modelled as a duct (3.1) without friction for positive flow rate. Negative flow rates are not allowed and the check valve closes. The resulting equations are:

$$\begin{aligned} L\dot{w} &= A_{in}p_{in} - A_{out}p_{out}, && for\ w > 0 \\ \dot{w} &= 0, && for\ w = 0. \end{aligned}$$

This can be implemented by setting the lower limit for the Simulink® integrator like zero.

3.8 Control valve

According to Egeland and Gravdahl (2002) the flow through a restriction or orifice in a valve when turbulent is

$$q = C_d A \sqrt{\frac{2}{\rho} \Delta p} \tag{3.28}$$

where Δp is the pressure drop over the orifice and C_d is a discharge coefficient.

To express the flow as mass flow w we use

$$q = \frac{w}{\rho}.$$

This can be inserted into (3.28) thus

$$\begin{aligned} \frac{w}{\rho} &= C_d A \sqrt{\frac{2}{\rho} \Delta p} \\ w &= C_d A \sqrt{2 \rho \Delta p}. \end{aligned}$$

We assume the variations in inlet pressure and temperature are relatively small hence ρ is constant. The mass flow through the valve is then given

$$w = C_v \sqrt{\Delta p}, \tag{3.29}$$

where $C_v = C_d A \sqrt{2\rho}$.

The mass flow through the control valve can be controlled between 0 and 100%. Let $C_v = C_v(l)$ be a function of valve stroke l where $C_v(l)$ is the valve characteristic and l is given as percent.

Let l_{set} denote the valve stroke set point. The valve response time is denoted t_{td} and represent the time between the valve set point is changed until the valve stroke l starts changing. The valve rise time is denoted t_r and represent the time between the stroke l starts changing until it has reached 67 % of its desired value. The dynamics of the valve stroke is then given

$$\dot{l} = \frac{1}{t_r}(l_s(t - t_{td}) - l) \tag{3.30}$$

where $l_s(t - t_{td})$ represents the stroke set point with a time delay t_{td}. This is implemented as a transport delay in Simulink®.

During the expansion the temperature will drop. We assume adiabatic expansion hence

$$\frac{T_2}{T_1} = \left(\frac{p_2}{p_1}\right)^{\frac{\kappa - 1}{\kappa}}. \tag{3.31}$$

3.9 Recycle line

The recycle line connects the compressor outlet with the cooler inlet, and the flow through the line is controlled with the recycle valve. As for the compressor, we assume no mass accumulation in the ducts and uniform flow over the entire length. The resulting control volume integral from (3.1) is

$$\frac{\mathrm{d}}{dt}\int_V \rho C\, dV = A_{in}p_{in} - A_{out}p_{out} - F, \tag{3.32}$$

where F represent the recycle valve friction. Note that the sign before F is minus in this case. This is because the valve is a passive component and represents a friction force against the flow. The resulting flow dynamics is

$$L\dot{w} = A_{in}p_{in} - A_{out}p_{out} - F. \tag{3.33}$$

At steady state, $\dot{w} = 0$ hence

$$A_{in}p_{in} - A_{out}p_{out} - F_{rv} = 0. \tag{3.34}$$

Further assuming that $A_{in} = A_{out} = A$ and inserting from (3.29) gives

$$\begin{aligned} A\frac{w^2}{C_v(l)^2} - F &= 0 \\ F &= A\frac{w^2}{C_v(l)^2} \end{aligned} \tag{3.35}$$

that gives the resulting flow dynamics

$$L\dot{w} = A\left(\Delta p - \frac{w^2}{C_v(l)^2}\right). \tag{3.36}$$

Note that this function is singular for $C_v(l) = 0$. This singularity can be avoided in simulation by adding a very small constant ϵ to $C_v(l)$ resulting in a small (neglectable) leak flow.

3.10 Upstream vessel

The upstream vessel will be modelled as a large volume using the vessel module resulting in (3.5) and (3.8).

3.11 Downstream vessel

We assume that the downstream vessel, which represents the entire processing plant downstream of the compressor, is very large and has very slow dynamics compared to the compressor system. The downstream vessel is therefore modelled as a reservoir with constant pressure. This is a reasonable assumption since the compressor system is a small part of the entire processing plant.

3.12 Gas turbine

The gas turbine generates power by expanding the air from the combustor. According to Moran and Shapiro (2000, p. 281-282) turbines have an isentropic efficiency between 70 and 90%. Figure 3.12 shows entropy-enthalpy diagram for the turbine expansion, where the inlet conditions are denoted 1, the outlet 2, and 2s denotes the outlet state for a perfect adiabatic expansion. Due to losses the turbine shaft power corresponds to the reduction in enthalpy between 1 and 2 hence

$$\begin{aligned} P &= w(h_1 - h_2) \\ &= wc_p(T_{in} - T_{out}). \end{aligned} \tag{3.37}$$

Inserting from (C.5) gives

$$P = wc_pT_{in}\left[1 - \left(\frac{p_{out}}{p_{in}}\right)^{\frac{(\kappa-1)\eta_\infty}{\kappa}}\right], \tag{3.38}$$

where the polytropic efficiency is denoted η_∞. The relation from (C.5) can also be used to determine the turbine outlet temperature when inlet temperature and pressure ratio is known:

$$T_{out} = T_{in}\left(\frac{p_{out}}{p_{in}}\right)^{\frac{(\kappa-1)\eta_\infty}{\kappa}}. \tag{3.39}$$

Note that this efficiency coefficient takes friction losses due to irreversibility into account, and not due to heat losses to the environment. We assume the heat losses are small such that they can be neglected.

To model the turbine mass flow, Kim et al. (2001) suggest using the Stodola equation

$$w = K\frac{p_{in}}{\sqrt{T_{in}}}\sqrt{1 - \left(\frac{p_{out}}{p_{in}}\right)^2}, \tag{3.40}$$

where K is a design specific parameter that can be found from experimental turbine data.

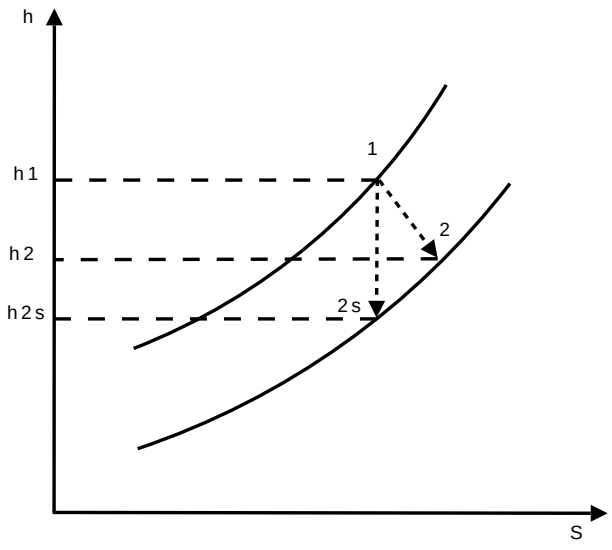

Figure 3.12: Turbine expansion entropy-enthalpy diagram.

3.13 Combustor

The combustor is a volume with two in flows, air and fuel gas. The air comes from the compressor and fuel is added as a mass flow. The combustion of the fuel is modelled as heat added to the volume. The heat added is found from the HHV, which is described in Section 2.8, of the natural gas.

The burner is a fixed control volume and we use mass and energy balance. From (B.1) we get

$$\frac{\mathrm{d}}{dt}m = w_{in} - w_{out}, \tag{3.41}$$

where $w_{in} = w_{in,air} + w_{in,fuel}$. The energy balance is given in (B.3). The work done by the system $\dot{W}$ is zero. We also assume that thermal energy dominates kinetic and potential energy. The resulting energy balance is

$$\frac{\mathrm{d}}{dt}U = w_{in,air}h_{in,air} + w_{in,fuel}h_{in,fuel} - w_{out}h_{out} + \dot{Q}, \tag{3.42}$$

where E is the control volume energy and $\dot{Q}$ is the heat added during combustion. The added heat is given

$$\dot{Q} = w_g\eta_c HHV, \tag{3.43}$$

where η is the combustors efficiency. Let $U = mu = mc_vT$ and $h = c_pT$ and insert into (3.42):

$$\frac{\mathrm{d}}{dt}(mc_vT) = w_{in,air}c_{p,air}T_{in,air} + w_{in,fuel}(c_{p,fuel} + \eta HHV) - w_{out}c_pT, \tag{3.44}$$

where $c_{p,air}$ is the specific heat for air, $c_{p,fuel}$ the specific heat for the fuel gas and c_v and c_p the specific heats for the gas mixture in the combustor. The specific heats are function of temperature and their variations can be found in Moran and Shapiro (2000, p. 838). How to deal with these variations will be treated in Section 4.6.4.

The energy balance in (3.44) can be rearranged and we get

$$c_v(\dot{m}T + m\dot{T}) = w_{in,air}c_{p,air}T_{in,air} + w_{in,fuel}(c_{p,fuel} + \eta HHV) - w_{out}c_{p,out}T. \tag{3.45}$$

Inserting (3.41) into (3.45) and rearranging gives

$$\begin{aligned}\dot{T} = \frac{1}{m}\Bigg[&\left(\frac{c_{p,air}}{c_v}T_{in,air} - T\right)w_{in,air} \\ &+ \left(\frac{c_{p,fuel}T_{in,fuel} + \eta HHV}{c_v} + T\right)w_{in,fuel} - \left(\frac{c_{p,out}}{c_v} - 1\right)Tw_{out}\Bigg].\end{aligned} \tag{3.46}$$

3.14 Shaft

The shaft dynamics is modelled using Newton's second law for momentum

$$J\dot{\omega} = \sum \tau, \tag{3.47}$$

where J is the inertia of the shaft including the compressor and the drive. The shaft angular speed is ω, and $\sum \tau$ is the sum of torques acting on the shaft. For a compressor and turbine with common shaft we have

$$J\dot{\omega} = \tau_g - \tau_c - \tau_f, \tag{3.48}$$

where τ_g is the torque generated by the gas turbine, τ_c is the compressor torque and τ_f is the friction. Since the compressor and gas turbine shaft output is given as power P and not torque, we will modify the equation using $P = \tau\omega$. The friction is assumed linear such that $\tau_f = k_f\omega$ that gives

$$J\dot{\omega} = \frac{1}{\omega}(P_g - P_c) - k_s\omega, \tag{3.49}$$

where k_f is a shaft friction coefficient.

4 Model identification and validation

In a scientific perspective, it is impossible to confirm that a model is valid. According to Smith (2009) validation is *'the process of determining the degree to which a model is an accurate representation of the real world from the perspective of the intended model users'*. In this thesis, the term validation is used about confirming that the model is likely to be satisfying accurate within given limitations. In scientific work, it is common that a physical model is created in order to test a theoretical model, and measurement of physical values like pressure, temperature and flow are made to support model validation. In this thesis, we have no influence where to take measurement of the process. Measurement values are limited by available sensors on the installation.

In this section we will identify the value of constants defined in Section 3 based on data from plants where the compressor system and the gas turbine system are located. The compressor system will be validated against a compressor at Plant A and the gas turbine system against a turbine at Plant B. Some parameters are based on specifications and data sheet from the given installations, while other values can be found using measurement data from the actual process.

We also want to state under which assumptions the model is valid. Several of the components have a working area where their behaviour is well known, but as they leave this area the behaviour is unknown and sometimes also uninteresting for this study.

The compressor system model structure is shown in Figure 3.1 and all modules are derived in Section 3. In this section the model parameters will be identified to fit data from a real compressor system both transient behaviour and steady state. The available measurement values are:

p_{sc}	Scrubber pressure / Compressor upstream pressure.
T_{sc}	Scrubber temperature / Compressor upstream temperature.
w_{cu}	Compressor upstream flow.
p_{cd}	Compressor downstream pressure.
T_{cd}	Compressor downstream temperature.
ω_{sh}	Compressor speed.
T_m	Cooler inlet temperature.
T_{co}	Cooler outlet temperature.
l_{rl}	Recycle valve position.

All physical parameters will use subscripts as shown in Figure 3.1. The subscripts are described in Appendix E.

The parameter identification procedure will follow these steps:

1. Identify physical sizes and values from plant specifications.

2. Approximate charts based on experimental values from manufacturer, mainly compressor pressure ratio, efficiency and shaft power.

3. Identify physical parameters like gas constants and specific heats based on specification and table lookup values.

4. Adjust uncertain physical parameters based on dataset of measurement.

5. Fit simulated steady state values against measured values.

6. Fit simulated transients against measured transients.

The dataset used for testing is from a two stage gas recompressor at Plant A. We have modelled and simulated the second stage. The first and the second stage have an almost identiacal structures. The first stage compresses from 5 to 32.2 bar, while the second stage from 32.2 to 85 bar. The two compressor has a commond drive and they will therefore have the same speed.

4.1 Compressor

The compressor module has three physical parameters, L_c, A_c and V_c, where L_c represents the equivalent length of the ducts including the compressor. The equivalent lenght is the distance a particle travels from the entrance of the duct, through the compressor and till the exit of the compressor downstream duct. This distance is somewhat longer than the physical distance between inlet and outlet because of the particles rotational trajectory inside the compressor. The duct outlet cross section area is denoted A_c, and is according to specification $A_c = \frac{\pi D^2}{4} = \frac{\pi 0.25^2}{4}$. The compressor equivalent volume V_c is as for L_c a parameter that can not be measured directly from the compressor or downstream volume, but a volume that represent pressure dynamics. We also know that this volume is by design small to be able to reduce downstream pressure fast to avoid surge in critical situations. Simulations show that all three values are essential when simulating surge to get the right frequency for the oscillations, and the size of the volume is also important for fast changes in the recycle valve when the check valve is closed since it tells how fast the pressure will drop at the compressor outlet. However, when the compressor is running steady state with continuous anti-surge control, these size represents much faster dynamics than the rest of the system such that their size is not of importance. For simulation $L_c = 10$ and $V_c = 3$ will be used.

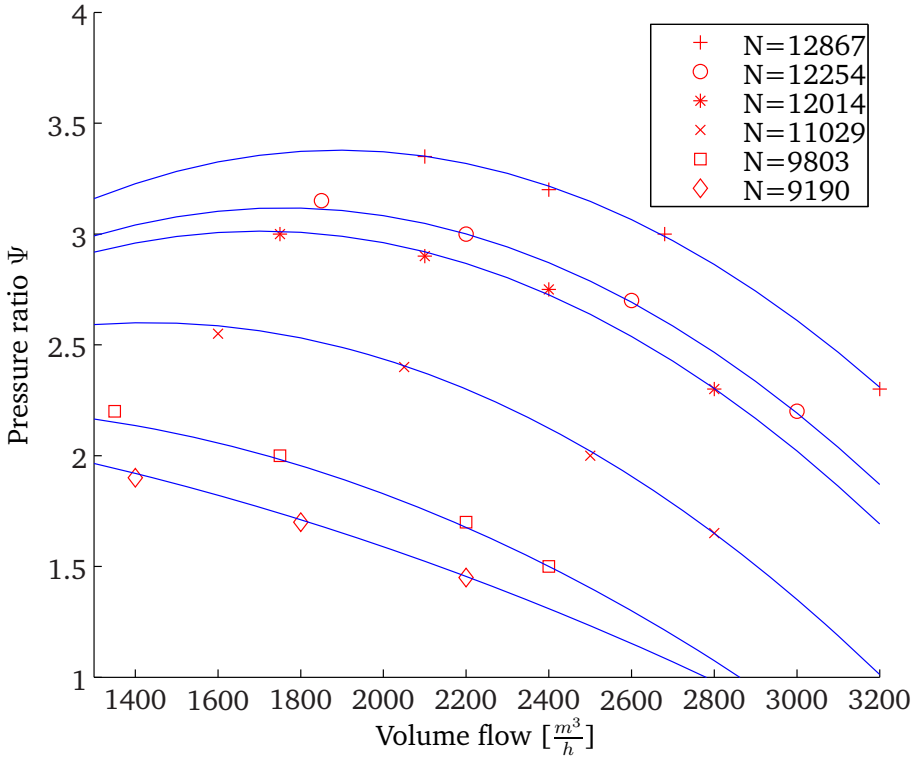

Figure 4.1: Compressor chart 2nd order polynomial fit excluding surge dynamics.

4.1.1 Compressor pressure chart characteristics

The compressor characteristic function were discussed in Section 3.3. The polynomial fit introduced in Section 3.3.1 will be used here to generate a function based on experimental compressor charts.

Figure 3.6 shows the compressor performance curves that have been approximated using 2nd and 3rd order curve fitting in Matlab®. The polynomial coefficients have been approximated using 3rd order curve fitting yet again as described in Section 3.3. Figure 4.1 shows the different speed curves in the compressor chart where the speed N is given in rpm. The red points represents points read from the chart in Figure 3.6 and the blue lines are the corresponding curves generated with the polynomial. The implemented function is available on enclosed CD in Appendix A.

Figure 4.2 shows corresponding curves using 3rd order polynomial. The curves have been extended by adding an extra point for no flow and negative flow for each speed curve such that the model also can simulate surge dynamics as described in Gravdahl and Egeland (1998, p. 501-504). However, the curves with surge dynamics have poor precision in the area to the right of the surge

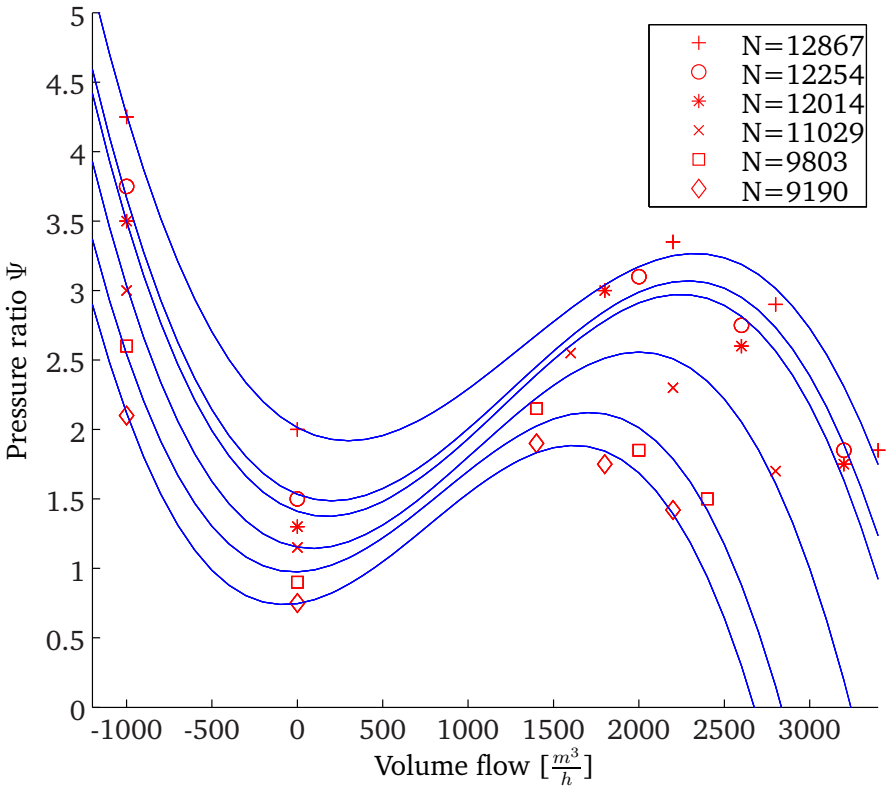

Figure 4.2: Compressor chart 3rd order polynomial fit including surge dynamics.

line, and the surge line has been moved to the right compared to the original chart in Figure 3.6. The result of this is that the simulated compressor can enter surge to early compared to the real compressor. The curves for the second order polynomial fit in Figure 4.1 will be used further. However, this function will limit the compressor model to be valid for operating on the right side of the surge line only.

The compressor chart that have been used represents pressure ratio as a function of volume flow q and compressor speed N. According to CCC the compressor chart is invariant with respect to pressure when represented for volume flow. However, we want to model the system using mass flow as physical parameter. When using the compressor chart the mass flow has to be casted to volume flow for the current inlet conditions.

The conversion from volume flow q to mass flow w is described in Section 3.3. According to the compressor manufacturer the compressibility factor at the inlet is $z_c = 0.891$ and the molar weight $M_{gas} = 21.97 \cdot 10^{-3}$. The anti-surge valve datasheet use $M_{gas} = 22.03 \cdot 10^{-3}$. In this thesis $M_{gas} = 22.00 \cdot 10^{-3}$ will be used for natural gas.

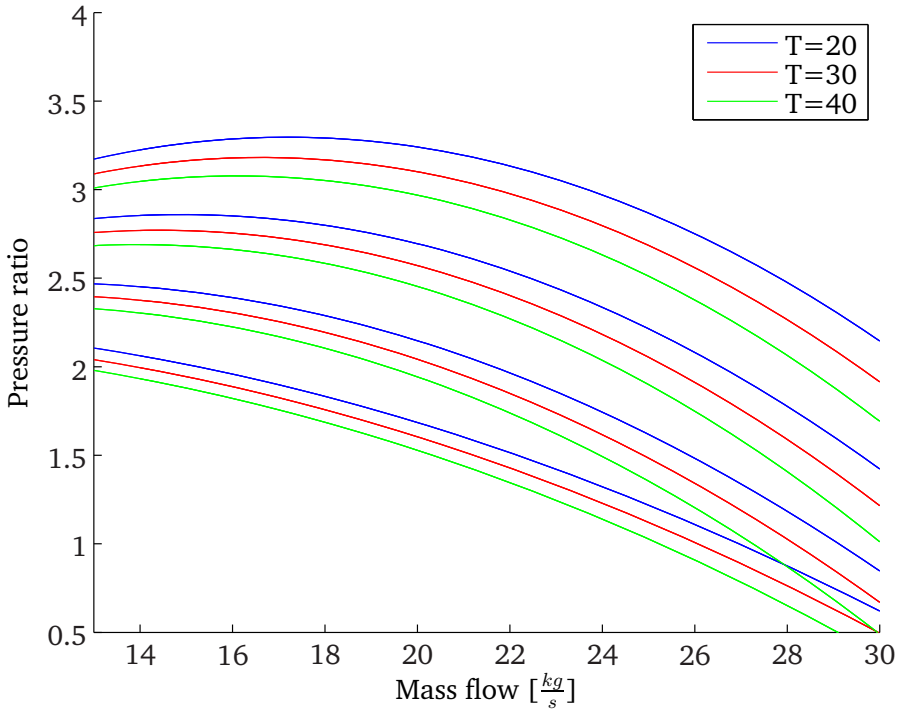

Figure 4.3: Compressor pressure ratio chart for varying temperature.

The compressor chart will vary with respect to temperature and Figure 4.3 shows the compressor chart for three different temperatures. All curves are ploted with inlet pressure $p_{cu} = 3.4 \cdot 10^6 Pa$ and compressibility factor $z_c = 0.891$. The compressor inlet temperature in the experienced data has to small variations to verify these variations, but it is an interesting property since increasing the inlet temperature is a method used for surge avoidance (Gravdahl, 2001).

4.1.2 Compressor efficiency chart characteristics

The compressor efficiency chart represents efficiency as a function of volume flow q and compressor speed N under the same conditions as for the pressure ratio chart. We assume this chart also is invariant with respect to pressure when represented for volume flow. The mass flow is casted into volume flow as for the pressure chart.

Figure 4.4 shows the values read from the efficiency chart in red, and the approximated values are shown in blue. As for the pressure ratio curves, the efficiency curves are valid only on the right side of the surge line, and only within the values showed with red in the figure.

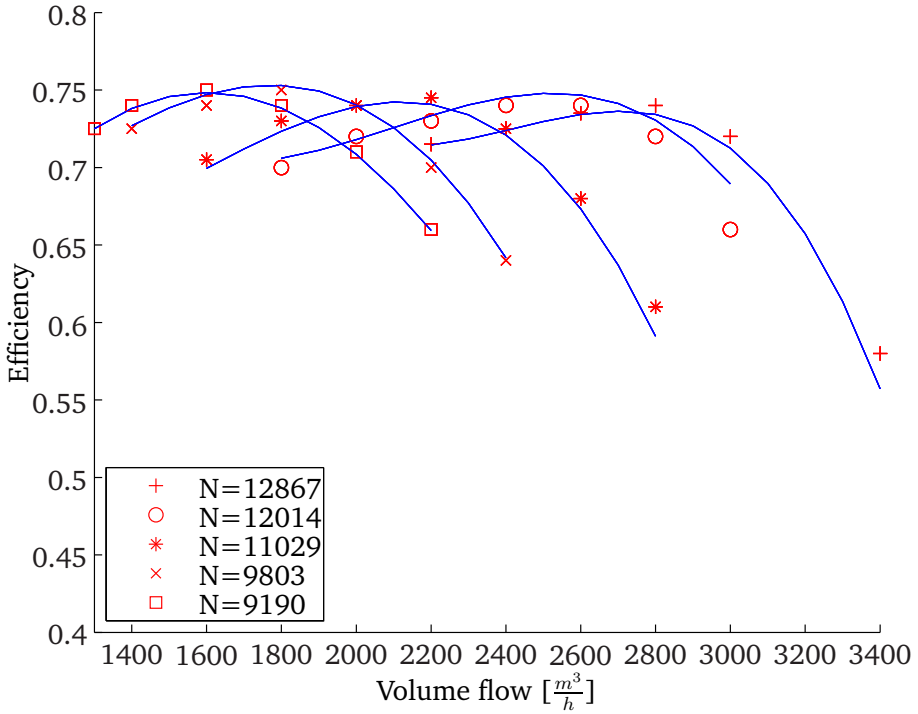

Figure 4.4: Compressor efficiency chart polynomial fit.

4.1.3 Compressor shaft power chart characteristics

The compressor shaft power is represented as a chart using polynomial fit on manufacturer experimental data. The result of the polynomial fit is shown in Figure 4.5. Values read from the efficiency chart in Figure 3.8 is marked with red and the approximated values in blue. The function has the same criteria for validity as for pressure ratio and efficiency.

4.1.4 Compressor outlet temperature

The relation between inlet and outlet temperature and pressure is given by (3.13). The polytropic efficiency η_c is given by the efficiency function Φ. According to *Engineering toolbox* (2009) $\kappa = 1.32$ for natural gas, while Plant A specifications uses both $\kappa = 1.264$ and $\kappa = 1.23$. Natural gas composition varies between different installations. Measurement of the compressor inlet temperature, inlet pressure and outlet pressure is used to find outlet temperature using (3.13). The different outlet temperatures has been compared with the measured value in Figure 4.6. The plot shows that $\kappa = 1.233$ gives a good fit, and this value will be used for natural gas further in the simulation.

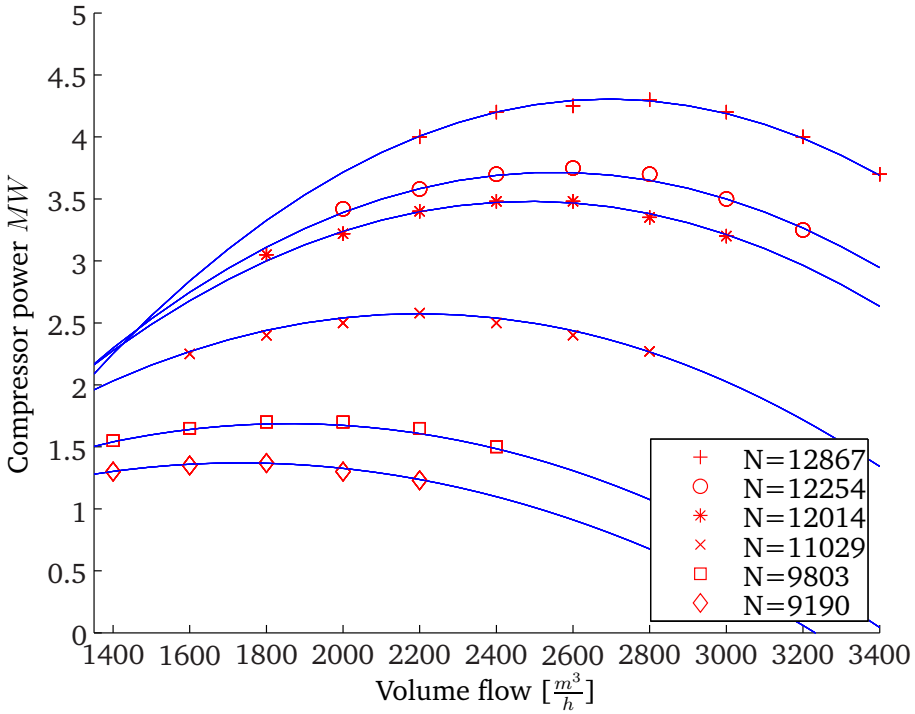

Figure 4.5: Compressor shaft power chart polynomial fit.

UH	773.66
A_{co}	280.504
V_{cold}	1.4472
V_{warm}	1.3126

Table 4.1: Cooler physical parameters.

4.2 Scrubber

The scrubber volume is according to Plant A specifications $V_{sc} = 2.0m^3$. Note that this model does not include liquid drained in the scrubber, which represents reduction in mass flow, energy and molar weight.

4.3 Cooler

The cooler data sheet for Plant A gives several of the physical parameters for the cooler. The values are shown in Table 4.1.

The cooling medium is water and $c_{p,c} = c_{v,c} = 4180$ in liquid phase. The cool-

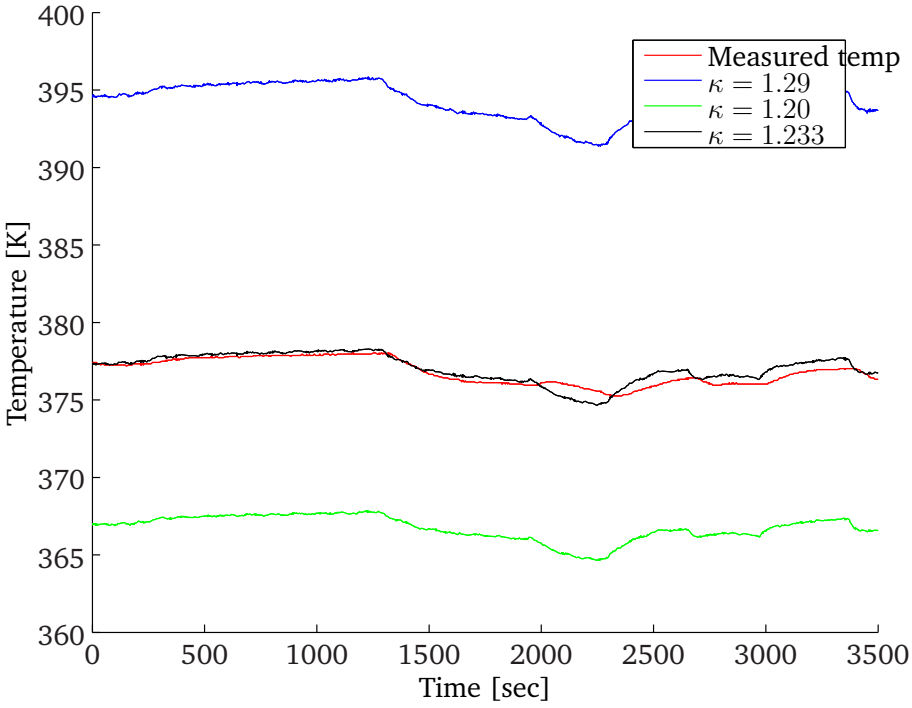

Figure 4.6: Compressor outlet temperature for different kappa values.

ing medium inlet temperature is $T_{cold,in} = 20°C$. According to process data, the natural gas is cooled from $85°C$ to $25°C$. We want to find the specific heat capacity, c_p, for natural gas in this range. Heat exchanger process data sheet operates with $c_{p,gas,25°C} = 2.32\frac{kJ}{kg}$ and $c_{p,gas,130°C} = 2.49\frac{kJ}{kg}$ between 30 and $130°C$. We choose the average temperature for the cooler, $55°C$ and find that $c_{p,gas,55°C} \approx 2.37\frac{kJ}{kg}$ when c_p increases proportional with temperature.

4.3.1 Cooler controller

The PI-controller structure is given

$$u = GK_p\left(e + \frac{1}{T_i}\int e\,dt\right), \tag{4.1}$$

where

$$G = \frac{u_{max} - u_{min}}{y_{max} - y_{min}}. \tag{4.2}$$

In this case $u_{max} = 100$ and $u_{min} = 0$, and $y_{max} = 220$ and $y_{min} = -50$ hence $G = \frac{100}{270}$. Further $K_p = 1$ and $T_i = 30$, which are values used at Plant A. Since the

controller output is saturated it is implemented with anti windup as described in the modelling section.

4.3.2 Cooler control valve

The cooler control valve has according to its data sheet linear characteristic. To determine the flow for 100% valve stroke, measurement from the process is used. Figure D.1 shows process values for gas inlet and outlet temperature, cooling medium outlet temperature, gas flow and valve stroke. We also know that cooling medium inlet temperature is $25°C$. When the valve stroke is 100%, we see that $T_{w,in} = 88°C$, $T_{w,out} = 25.5°C$, $T_{c,out} = 38°C$ and $w_w = 20\frac{kg}{s}$. By further assuming no loss of heat to the environment the steady state gas flow w_c is given by

$$\Delta T_w c_{p,w} w_w = \Delta T_c c_{p,c} w_c \tag{4.3}$$

which gives $w_c = 39.3\frac{kg}{s}$. We assume the cooler control valve has a maximum capacity of approximately $w_{c,max} = 40\frac{kg}{s}$ for full valve stroke. The inlet and outlet pressure is constant and the ratio between flow and valve stroke is constant and linear. The valve stroke opening time is $t_{tv} = 12sec$. The resulting flow dynamics for the cooling medium is

$$w_c = \frac{w_{c,max}}{100} l_{tv} \tag{4.4}$$

$$\dot{l}_{tv} = \frac{1}{t_{tv}}(l_{tv,set} - l_{tv}), \tag{4.5}$$

where l_{tv} is percent position of the temperature valve stroke and $l_{tv,set}$ is the set point given by the controller.

4.3.3 Validating on dataset with variable flow and temperature

The number of interconnected heat exchanger elements n also has to be chosen. For an ideal counter flow heat exchanger, n tends to infinity. By reducing n the heat transfer rate is reduced. The cooler is a shell and tube heat exchanger, and not purely counter flow. We seek to find the n value giving heat exchanger behaviour close to process data values.

Figure D.2 shows the test setup used in Simulink®, and Figure D.3 and Figure D.4 shows the resulting simulation with $n = 4$ and $n = 6$ respectively. It is obvious that the cooler is more efficient with $n = 6$ since it uses full valve stroke for a shorter time, and it also gives closer valve characteristic to the dataset. However, the main reason for choosing $n = 6$ is that it gives best fit for the gas outlet temperature.

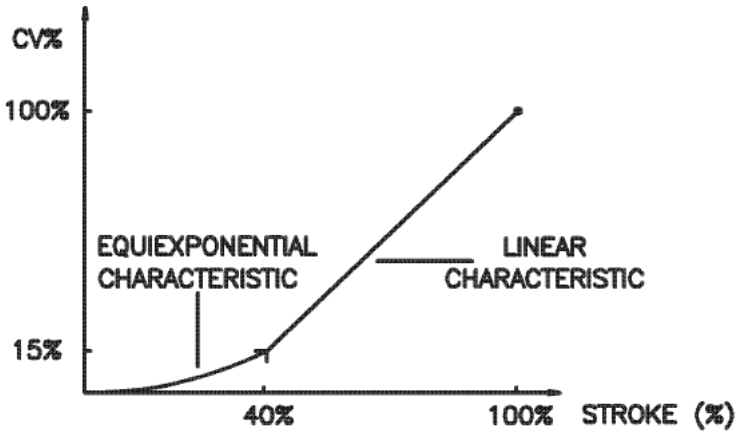

a: Anti-surge valve characteristics from datasheet.

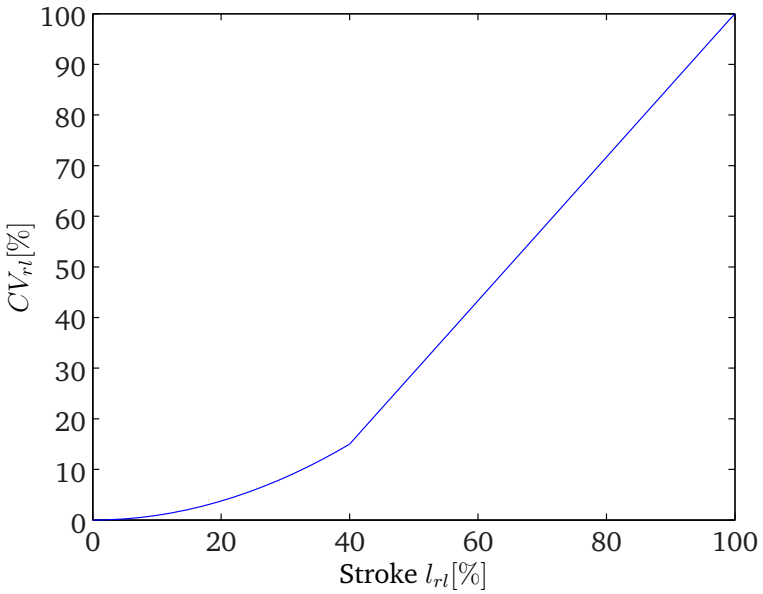

b: Anti-surge valve modelled characteristics.

Figure 4.7: Anti-surge valve characteristics.

4.4 Recycle line

Figure 4.7a shows the anti-surge valve characteristic that can be approximated using

$$C_{v,rl}(l_{rl}) = C_{v,rl,max}\left(\frac{15}{16}l_{rl}^2\right), \qquad \text{for } l_{rl} \in (0, 40\%),$$
$$C_{v,rl}(l_{rl}) = C_{v,rl,max}\left(\frac{17}{12}l_{rl} - \frac{5}{12}\right), \qquad \text{for } l_{rl} \in (40, 100\%), \tag{4.6}$$

where $C_{v,rl,max}$ is the maximum flow coefficient for full stroke, $l_{rl} = 100\%$. Figure 4.7b shows the characteristics for the approximation in (4.6).

The recycle valve specifications show that for $\Delta p_{rl} = 5.51MPa$ the flow is $w_{rl} = 20.84\frac{kg}{s}$. Let $C_{v,rl,max} = \frac{w_{rl}}{\sqrt{\Delta p_{rl}}} = 8.85 \cdot 10^{-3}$. The model structure is given in Section 3.8.

The rise time $t_{r,rl} = 2sec$ and response time $t_{td,rl} = 0.3sec$ are both given by specifications. They can be inserted into (3.30) to get the valve stroke dynamics.

The recycle line length is chosen $L_{rl} = 100m$ and the diameter $D_{rl} = 0.25m$.

4.5 Overall compressor system

Unfortunately, there are not pressure, flow and temperature measurement between each element in the process. Some assumptions are necessary to test the overall compressor system. Process data will be used as input for recycle valve stroke, compressor speed and downstream vessel pressure that is constant. There is no flow measurement of the upstream vessel inlet flow and this is assumed constant and chosen such that it gives a best fit with flow measurement in the compressor and simulated flow.

Figure 4.8 shows the input signal to the overall model for recycle valve position and compressor speed and Figure 4.9 shows the response. The downstream vessel pressure is $p_{dv} = 8.577 \cdot 10^6 Pa$ and testing shows that flow into the upstream vessel $w_{uv} = 8.5$ gives good fit to the dataset.

Figure 4.9 compares simulated and measured pressure, temperature and flow for the compressor for the given input. The simulation follows the dataset quite good, especially for temperature and flow. Between 4000 and 7000 sec, the simulated flow is somewhat lower than actual flow. Note that in this area, the compressor speed is higher. A higher compressor speed will also affect the first compressor stage, and the consequence is that the inlet flow and pressure to the second stage also increases. This can explain some of the deviation in the simulation.

In order to study the transients in the system, we want to study the response between 1000 and 4000 sec shown in Figure 4.10a and 4.10b. The figures represent the same response for two different upstream vessel volumes. For a large volume, the step response in the recycle valve (shown on the right y-axis) is more damped out than for a small volume. By comparing these figures we see that $V_{uv} = 200m^3$ give a better fit. Also note that the compressor speed is not kept constant for the response in Figure 4.10a and 4.10b, which makes it difficult isolate the response for a step in the recycle valve.

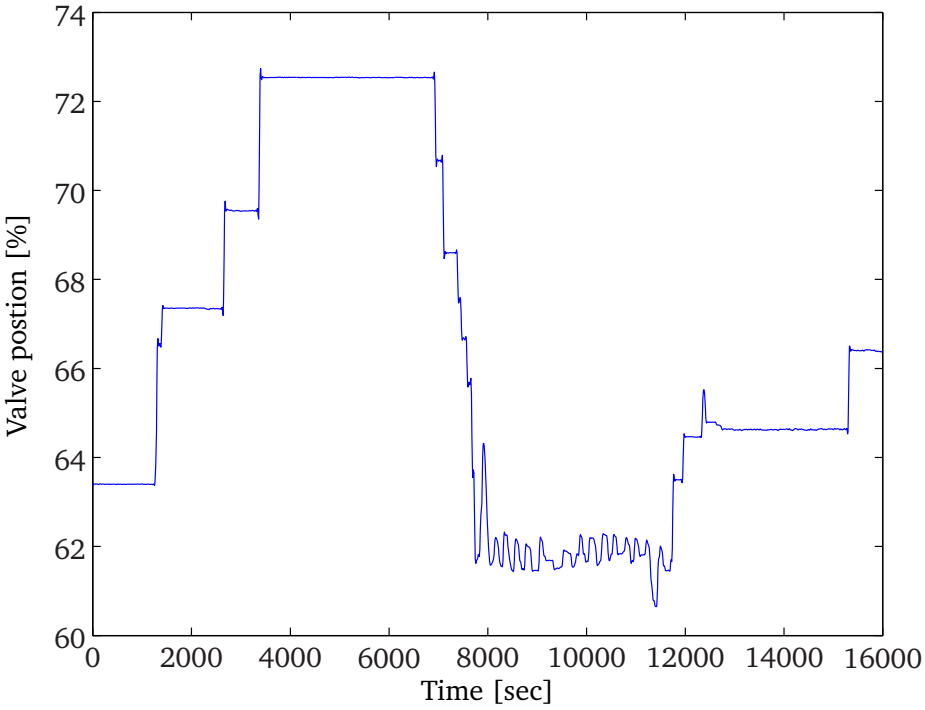

a: Valve position input.

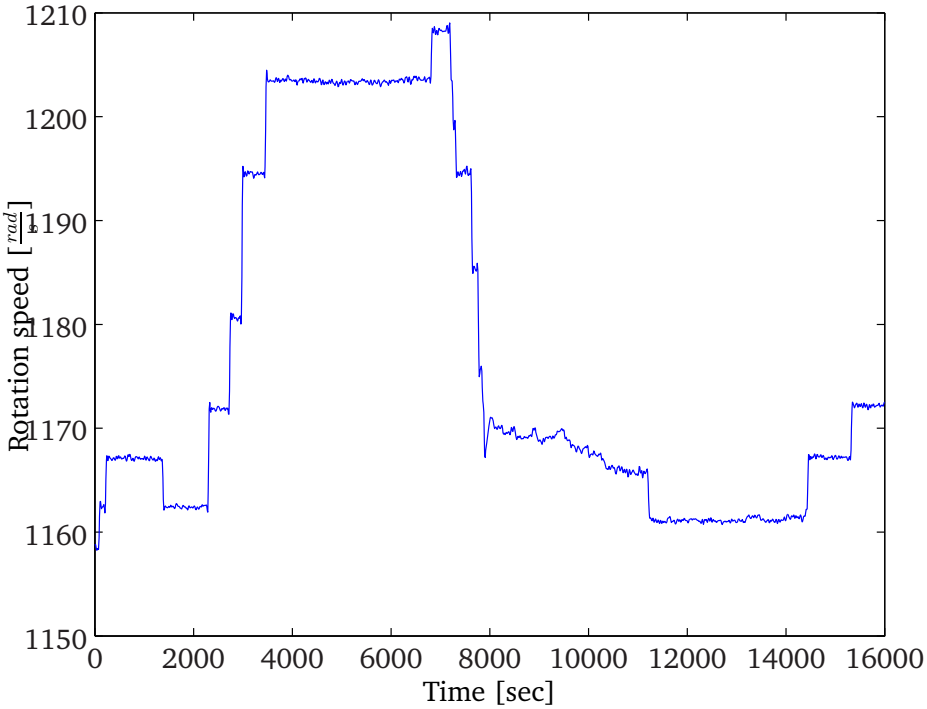

b: Compressor speed input.

Figure 4.8: Overall system simulation input.

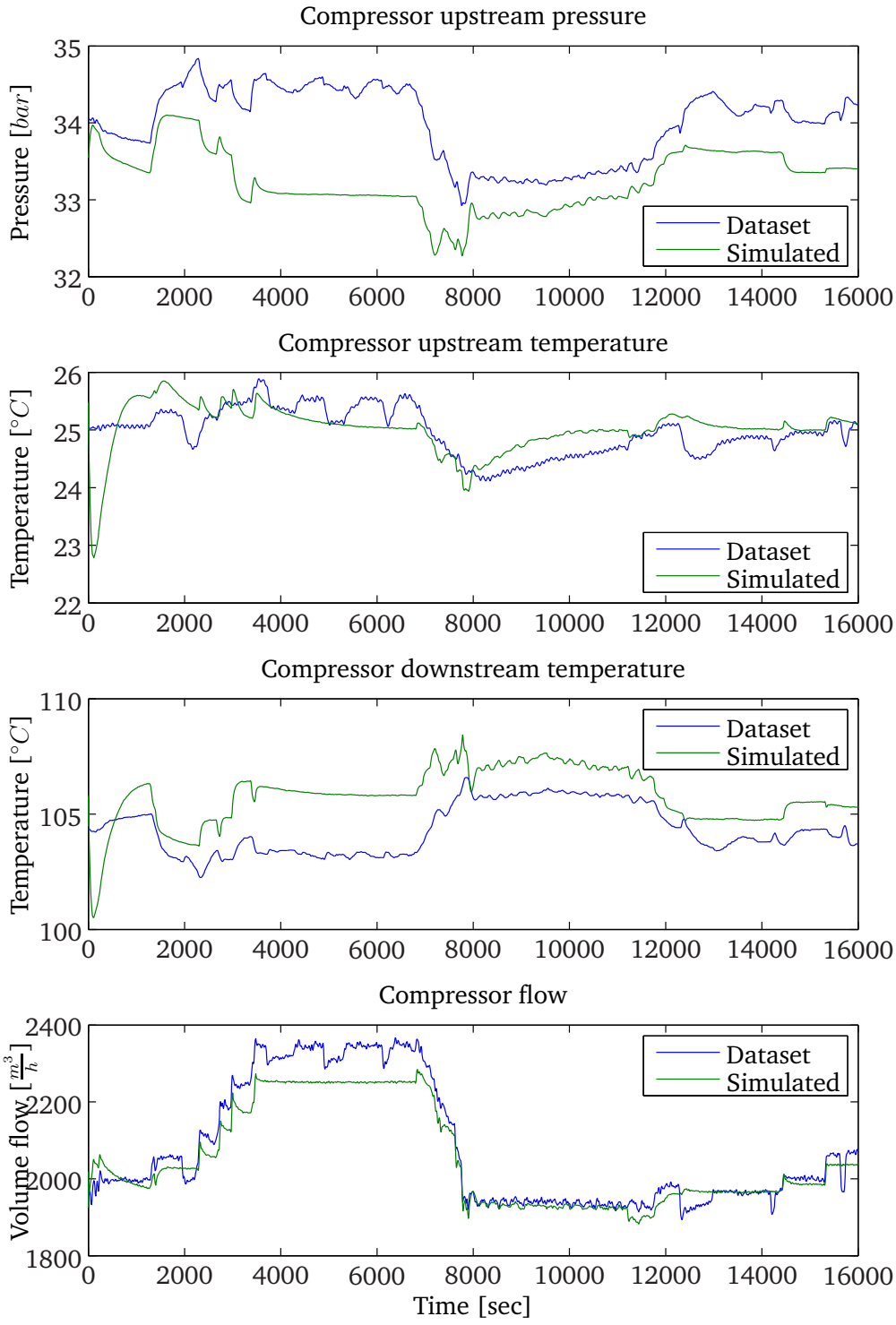

Figure 4.9: Simulation of compressor pressure, temperature and flow.

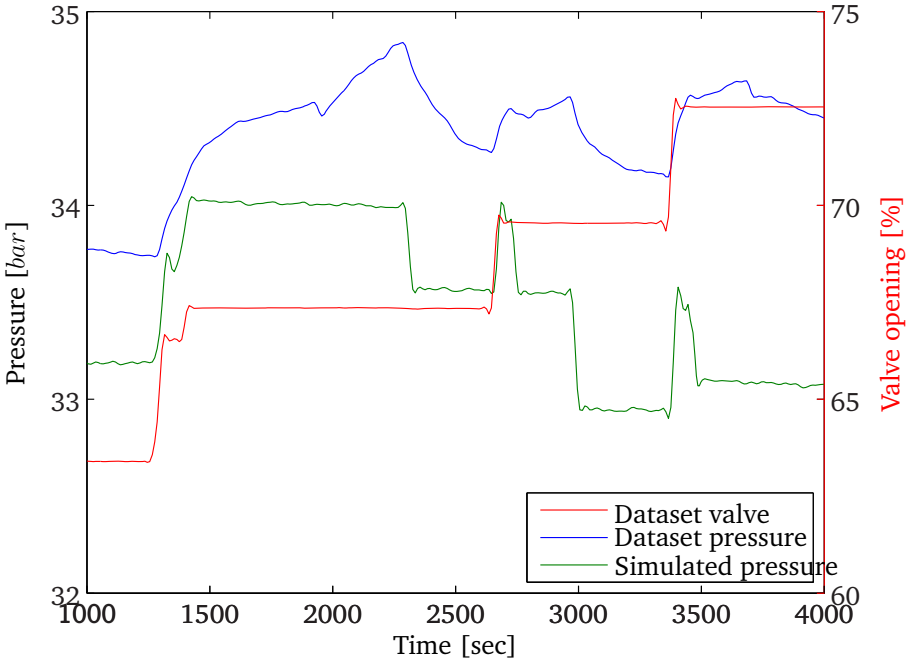

a: Upstream vessel volume $10m^3$.

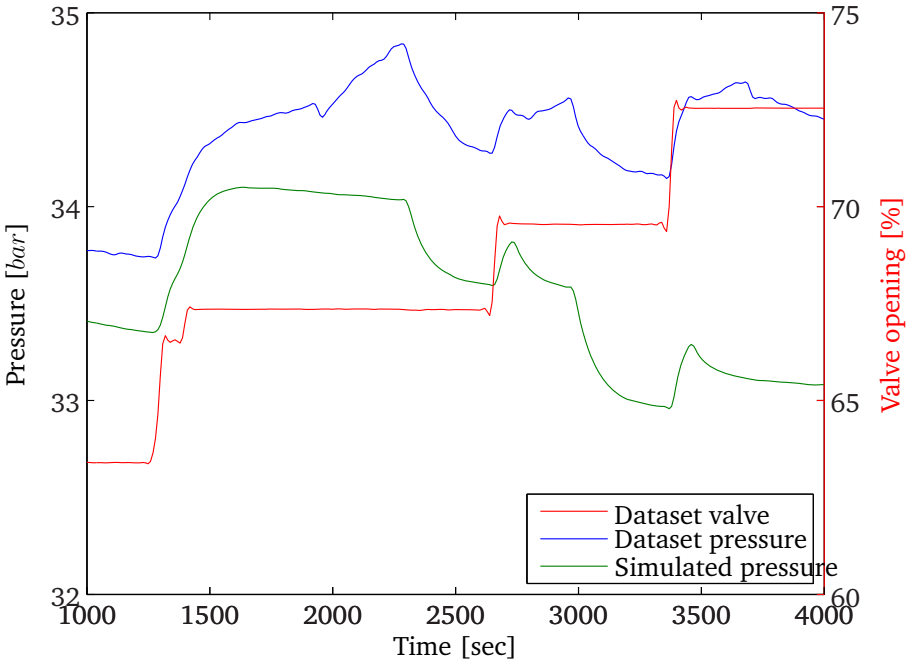

b: Upstream vessel volume $200m^3$.

Figure 4.10: Compressor upstream pressure dynamics for different upstream vessel volumes.

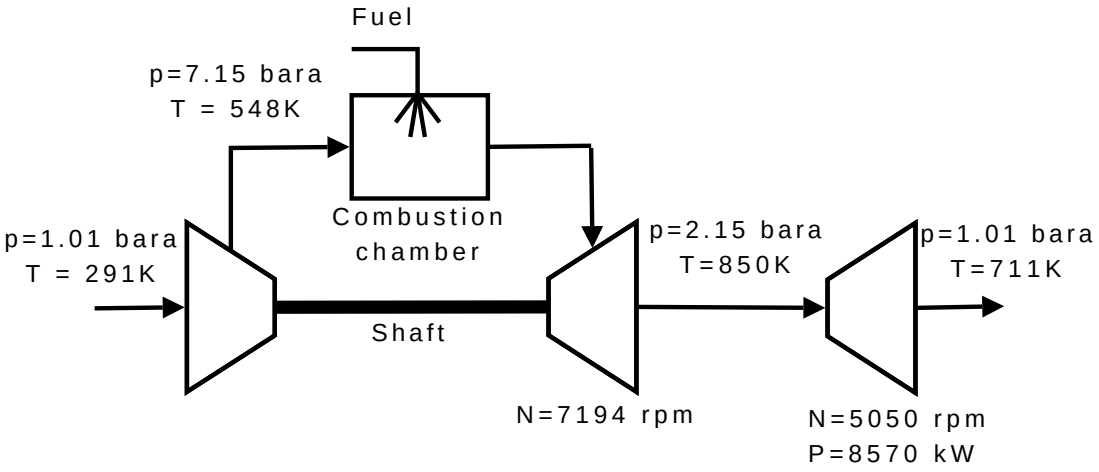

Figure 4.11: Turbine system measured steady state values.

4.6 Gas turbine system

Unfortunately, there are little turbine data available for identification of transient behaviour. Figure 4.11 shows the turbine system with the known measurement values at a given time for Plant B, and these values will be used to identify some of the gas turbine system parameters and initial values.

4.6.1 Power turbine

The temperature and pressure drop over the power turbine is known, and the shaft power is known. From (3.37) we want to find the mass flow through the power turbine. We assume the gas is air since the fraction natural gas added in the combustor is small, less than 1/50. We want to use specific heat for air at $T = 780K$, which is the average between power turbine inlet and outlet temperature. By using values from C.6, we get $c_{p,air,780K} \approx 1.093\frac{kJ}{kg}$. Similar for specific heat ratio we get $\kappa_{air,780K} \approx 1.357$. Mass flow through the power turbine is given

$$w_{pt} = \frac{P_{pt}}{c_{p,air,780K}(T_{in} - T_{out})},$$

where $P_{pt} = 8570kW$, $T_{in} = 850K$ and $T_{out} = 711K$. This gives $w_{pt} \approx 56.4\frac{kg}{s}$. Let us further use (3.39) to determine the polytropic efficiency η_{pt} of the turbine:

$$\eta_{\infty pt} = \frac{\ln \frac{T_1}{T_2}}{\frac{\kappa-1}{\kappa}\left[\ln\left(\frac{p_1}{p_2}\right)\right]},$$

which gives $\eta_{pt} \approx 0.90$. Note that this value represents the gas turbine efficiency, and not the gas turbine cycle efficiency.

Finally, we want to find the turbine mass flow parameter $K_{t,pt}$ using (3.40):

$$K_{t,pt} = \frac{w_{pt}\sqrt{T_1}}{p_1\sqrt{1-\left(\frac{p_2}{p_1}\right)^2}},$$

where all the values are given in SI-values; pressure in Pa and temperature in K. This gives $K_{t,pt} \approx 8.66 \cdot 10^{-3}$.

4.6.2 Turbine volume

The size of the volume between the turbines is unknown and in simulation $V_{tv} = 5m^3$ is used. The specific heat ratio for air in this module is $c_{p,air,850K} \approx 1.349$.

4.6.3 Gas turbine

We can further analyse the gas turbine as we analyzed the power turbine. We already know the mass flow through the turbine, and we also know the outlet conditions, which are the same as the inlet conditions for the power turbine. The combustion chamber is just a vessel where heat is added and the pressure is uniform thus the inlet and outlet pressure are equal. Let the gas turbine have the same polytropic efficiency as the power turbine such that $\eta_{\infty gt} = 0.90$. The temperature are higher here, and we use different values for c_p and κ. We assume the average temperature over the gas turbine is $1000K$, and $c_{p,air,1000K} = 1.142\frac{kJ}{kg}$ and $\kappa_{air,1000K} = 1.336$. The gas turbine inlet temperature is found from (C.5):

$$T_1 = T_2\left(\frac{p_1}{p_2}\right)^{\frac{(\kappa-1)\eta_{\infty gt}}{\kappa}}.$$

This gives $T_1 \approx 1116K$. Further the flow constant $K_{t,gt}$ is given such that

$$K_{t,gt} = \frac{w_{gt}\sqrt{T_1}}{p_1\sqrt{1-\left(\frac{p_2}{p_1}\right)^2}},$$

which gives $K_{t,gt} = 2.76 \cdot 10^{-3}$. The gas turbine power can be found using (3.37)

$$P_{gt} = w_{gt}c_{p,gt}(T_1 - T_2), \tag{4.7}$$

where $P_{gt} = 17.1MW$ in this case.

4.6.4 Combustor

The combustor is modelled as a vessel where heat is added through combustion of natural gas. According to Bossel (2003) the higher heating value for natural gas is $HHV = 42.5\ MJ$. We assume the added natural gas has the same temperature as the compressed air, and that the c_p and κ are unaffected since the natural gas fraction is small. The average temperature over the combustor is $T_{comb,avg} = 832K$. Interpolating the values from C.6 gives $c_{p,comb} = c_{p,air,832K} = 1.106\frac{kJ}{kg}$ and $\kappa_{comb} = \kappa_{air,832K} = 1.351$. Fuel added to the combustor is given by (3.43) hence

$$w_{fuel} = \frac{\dot{Q}}{\eta_{comb} HHV}, \tag{4.8}$$

where $\dot{Q} = w_{comb} c_{p,comb}(T_2 - T_1)$. This gives $w_{fuel} = \frac{884}{\eta_{comb}} \cdot 10^{-3} \frac{kg}{s}$. The choice of η_{comb} will only scale how much of the fuel is transferred into heat and will not be important in this model. For simplicity, $\eta_{comb} = 1$.

4.6.5 Compressor

Both inlet and outlet condition for the compressor is given. Average temperature $T_{comp,avg} = 420K$, which gives $c_{p,comp} = c_{p,air,420K} = 1.016\frac{kJ}{kg}$ and $\kappa_{comp} = \kappa_{air,420K} = 1.393$. Using (C.5) and temperatures as shown in Figure 4.11 gives $\eta_{comp} = 0.87$. This value is surprisingly high compared to the compressor in the process where $\eta_c \approx 0.73$. It is possible that this compressor is more efficient, but the difference can also be a result due to cooling or heat loss during compression. Deviation in specific heat and specific heat ratio values can also cause some error. There is no available information about compressor pressure ratio map, and we have to use map from another compressor and scale to fit this case. The compressor is running at $N = 7194rpm$ and the pressure ratio chart is shown in Figure 4.12 for compressor speed $\omega = 725 - 825rad/s$.

4.6.6 Step responses for turbine system

Figure 4.13 shows step response for the gas turbine for step in fuel and load. At 50 seconds the fuel is stepped from approximately $0.8kg/s$ to $1.0kg/s$, and at 100 seconds the load torque is stepped from 20 to $25kNm$.

Figure 4.14 shows simulated steady state values for atmospheric system inlet and outlet pressure and $w_{fuel} = 0.775kg/s$. Simulation show that the steady state values are quite close to the design values from Figure 4.11.

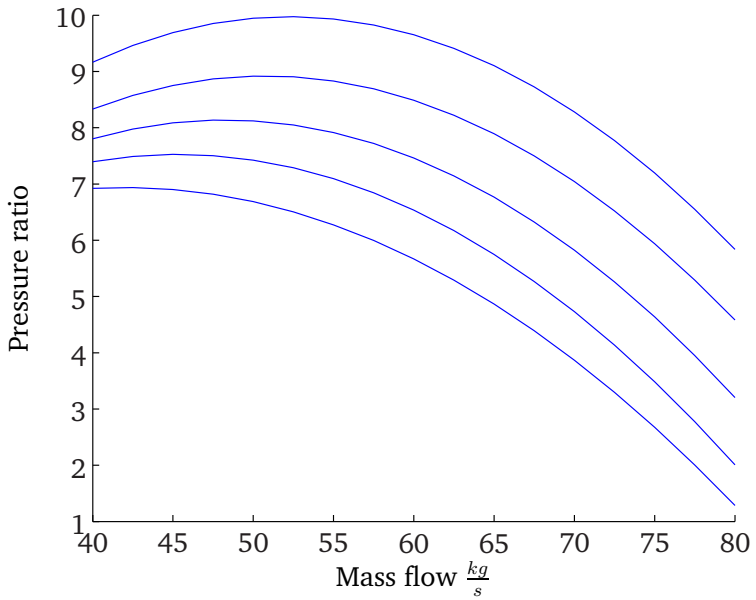

Figure 4.12: Compressor pressure ratio chart for the internal compressor.

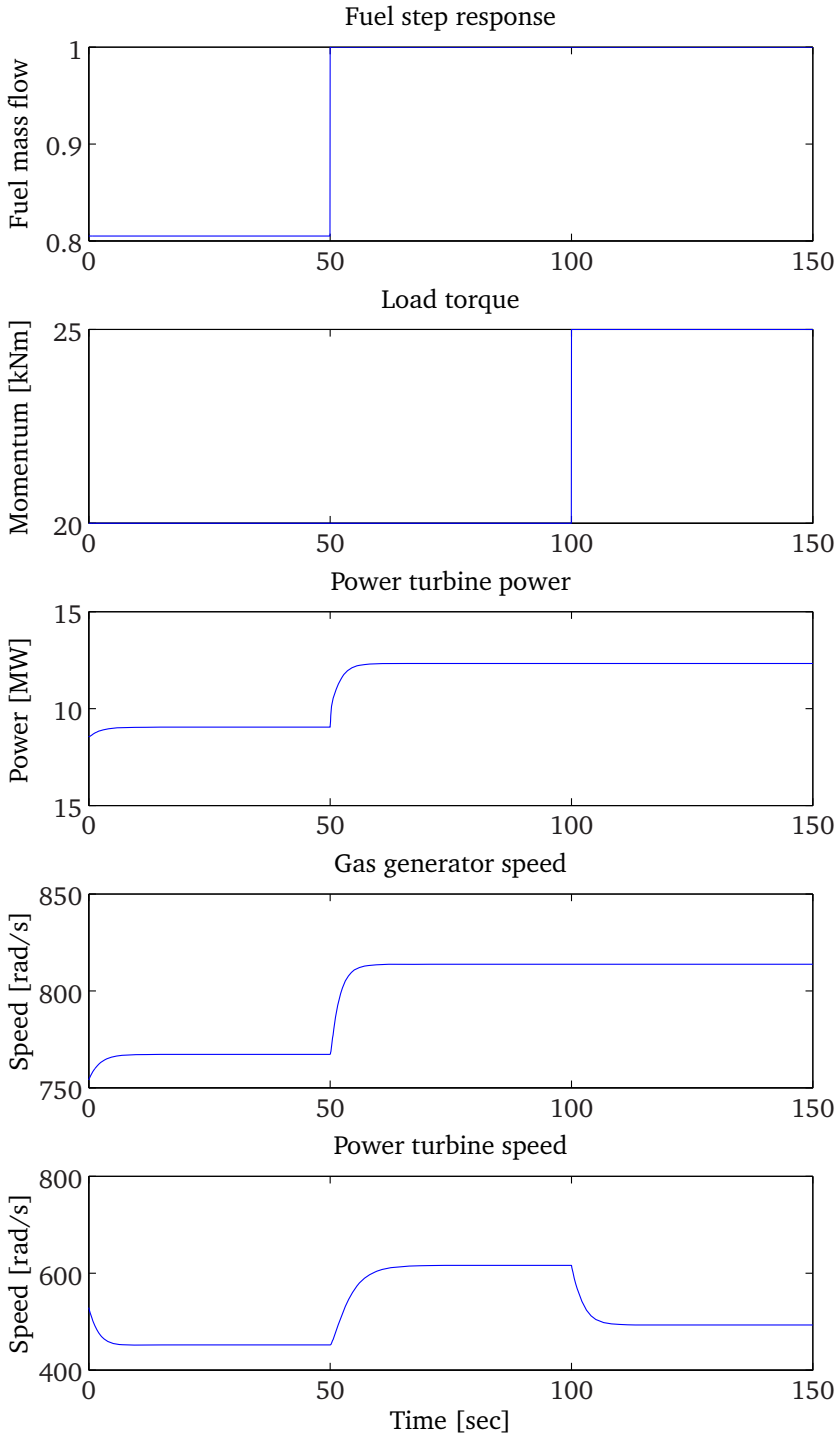

Figure 4.13: Gas turbine system step response.

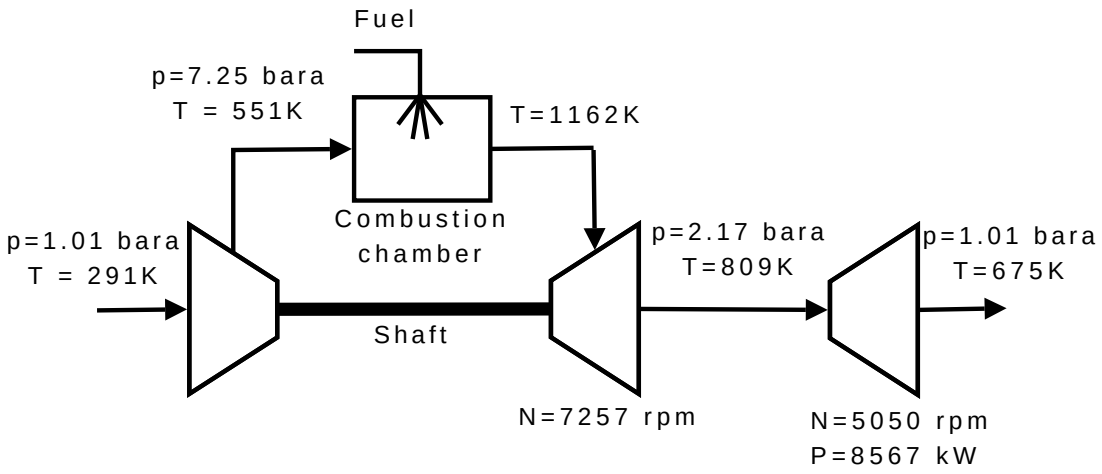

Figure 4.14: Turbine system simulated steady state values.

5 Model evaluation

The simulations in Section 4 show that the overall system response give a good fit to the dataset from Plant A. The simulated pressures increases and reduces synchronously with the dataset values, and similar with the temperature and flow. However, there are some deviations in steady state values. In this section we will have a closer look on each modules, the assumptions they rely on and what the consequences of these assumptions could be. We will also study the results from Section 4 and see if we can explain some of the deviations from these assumptions.

5.1 Compressor

The relation between pressure, flow and speed is given quite accurate for steady state by compressor maps. We have used the compressor maps for pressure, efficiency and shaft power. The results also show that the polynomial fit gives a rather good approximation of the maps. However, the compressor chart from the compressor manufacturer is valid only for given inlet conditions regarding pressure, temperature and gas composition. We have assumed that the volume flow compressor map is invariant with respect to pressure. But still we have to cast the flow from mass flow to volume flow to use the map that introduces a new source of error; ideal gas model. Even if we use a compressibility factor for correction, the ideal gas model is not quite accurate since the compressibility factor will vary with pressure, temperature and gas composition. Equivalent deviations will occur for the efficiency and shaft power map. The consequence of potential deviations is steady state bias for pressure, temperature, flow and shaft power.

We have also taken into account variations in compressor pressure ratio map for varying temperature. This is based on modelling from Egeland and Gravdahl (2002, p. 494) and is also used in Gravdahl (2001). Unfortunately, it is difficult to find sources that can confirm this effect based on experimental scientific work. The deviations in inlet temperature in the dataset are to small to evalute this effect.

The stated assumptions can cause small errors concerning pressure ratio, flow, temperature and shaft power for the compressor, but the qualitative behaviour is little affected. An increase in inlet flow will reduce the pressure ratio over the compressor, and an increase in speed will increase the pressure ratio for both dataset and simulation. The uncertainty in the model is related to how much it will change. The test results show that the simulated values are not far from the real values.

5.2 Duct

The duct module is used in all momentum balances. Compared to the other system components, its response is very fast and it can easily make the system stiff[3]. Simulations have shown that accurate initial values are very important, especially for pressures at inlet and outlet of the duct.

In the model, there is no friction in the duct modules, nor is there measurements that can be used to find friction coefficient for the pipes. The compressor adds a big amount of energy to the gas in the system, and the loss due to pipe friction will probably be small. This is also shown in Section 2.7. Moreover, the system is designed to reduce these losses since it reduces the payload efficiency of the system. However, friction can easily be added to the duct modules using the pipe friction model described in Section 2.7 or a more simple friction model like linear friction with respect to fluid velocity and pipe length or surface area.

The duct outlet temperature is directly connected to the duct inlet temperature and is a possible source of error, especially for abrupt temperature changes and long ducts. From the results of the step response, we see that the temperature transient has a rise time of several minutes. The error connected to this assumption it therefore very little. Different duct lengths have been tried in the compressor system, both for the compressor duct, the recycle line and the upstream duct. Variations between 1 and 100 meters did not give visible changes in the system response.

5.3 Manifold

The manifold is a mixing unit where we have excluded all dynamics. From the system dataset it is difficult to analyze how this module appears compared to the real system. There will probably be some friction due to turbulence in the mixing point. Since the compressor represents a very large energy source in the system, this loss will be as for all friction losses in the system relatively small.

5.4 Cooler

The cooler dynamics is essential for the compressor system behaviour regarding compressor inlet temperature. The volume of the cooler will give a delay from change in inlet temperature till change in outlet temperature. What will cause even more delay is the controller integral time, which is approximately

[3] A problem is stiff when there are large deviations in eigenvalues in the system. Stiffness can lead to oscillations in the simulation that slows down simulation time.

80 seconds. For slow changes the cooler will follow the reference temperature quite well, but from the results in Appendix D show that the cooler controller integral time gives a deviation in cooler outlet temperature of 1 degree for the dataset and 2 degrees for the simulated values. These temperature variations are relative small, but will affect the mass flow to volume flow conversion for the compressor where $q = \frac{zwRT}{p}$.

Another interesting observation made during simulation is that the compressor inlet temperature increases when the recycle valve is opened. However, this is not due to increase in gas temperature into the cooler, but due to increase in flow through the cooler. The cooler is unable to cool that big amount of gas for the current cooling fluid flow and takes time to adapt because of the integral time.

5.5 Scrubber

The scrubber continuously drains liquid from the cooled gas, and is according to its specifications able to remove up to 2865 kg/h liquid. For comparison the compressor compresses approximately 22 kg/s gas at steady state near its design point. These numbers indicate that up to 3.6% of the gas can be removed during scrubbing. The liquid drain is not taken into account in the model, and it represents both removal of mass and energy flow through the scrubber, and it also changes gas composition, which yet again changes molar weight and specific heats. Some of the error could be corrected by adding a constant drain in the scrubber. However, the liquid fraction in the cooler will vary depending on recycle valve position. The recycled gas is dryer such that the liquid draining mainly depend on system inlet flow and composition.

A more accurate way to model the scrubber is to introduce multiphase flow. This requires that all the modules in the entire models are modified. In the scrubber, a phase diagram for the specific gas is used to determine how much liquid is drained. Another benefit with multiphase flow is that it also allows for varying mole weight in the system. The mole weight will be higher before scrubbing.

The simplification of the scrubber does obviously introduce some deviation compared to the physical system, but lack of flow measurement makes it difficult to state how much. Since the amount of fluid drained is low, the simplification made in this model is acceptable.

5.6 Check valve

There is no dynamics in the modeling of the check valve open/close mechanism. It is modelled as an ideal check valve with no loss of pressure for open position. We are not able to verify the pressure drop from the process data. The valve allows no reversed flow and opens immediately when the differential pressure is positive. Simulations show that under normal operating conditions, $w_c \approx 18kg/s$, the check valve did not close even if the recycle valve was stepped from 0 to 100%. This indicates that the check valve is in use only for very rare cases like shutdown or surge, and is not of significance for continous surge avoidance control.

The check valve can be extended to include valve stroke dynamics where the valve not closes until there is reversed flow or negative differential pressure. In the simulation cases in this thesis the check valve does not close at all and its stroke dynamics is therefore of no interest for those cases.

5.7 Recycle line

The recycle valve controls the flow in the recycle line. System specifications give detailed information about recycle valve dynamics and characteristics, which have been implemented in the model. Lack of flow measurement in the recycle line makes more detailed system verification difficult.

Simulations for the overall system for different recycle valve positions has measurement of the compressor flow, and this gives a good indication of the recycle line model quality. Between 1000 and 4000, the valve steps from about 63% to 73%, and between 6000 and 8000 back to 62%. The compressor flow before and after the steps gives a very good fit, while between 4000 and 6000 the simulated flow is samewhat lower than expected. This can be due to modelling error in the recycle valve, but varying flow into the system can also contribute to the error.

5.8 Split

The split module is used to split up a flow from a volume and is just a model technical detail and requires no identification or validation.

5.9 Upstream vessel

Simulations showed that the upstream vessel size is of great importance to get the right transient behaviour for system pressure and temperature for recycle valve step. This indicates that the temperature and pressure transients mainly depend on how long it takes for the upstream system to change outlet pressure.

Remember that the upstream vessel for the dataset used here represents the first stage compressor system. The flow and pressure will depend on inlet pressure of the second stage compressor, compressor speed and upstream conditions. We have assumed constant upstream vessel inlet flow for all simulations. Both the first and second stage compressor is connected to the same governor. A change in speed will therefore affect the upstream vessel inlet flow, which has not been taken into account. However, this is not a weakness for the model, but a simplification due to the boundary conditions. For the given test data we can not state weather flow deviations are caused by the upstream conditions, the recycle line or other modules in the model. Nevertheless, it is likely that a change in compressor speed will have significant influence for the second stage inlet conditions.

5.10 Downstream vessel

This compressor system delivers 3-5% of the total gas flow to the downstream vessel, hence a small change in the flow will not affect its pressure noticeably. A pressure change in this vessel is mainly caused by other subsystems. The dataset used for comparison in the simulation also showed that the outlet pressure was constant.

5.11 Gas turbine system

The gas turbine system has several similarities to other gas turbine models for simulation like Reed (1993), Kim et al. (2001) and Camporeale et al. (2006). A comparison against real operating data is performed in Kim et al. (2001) and shows that the model give satisfying response at steady state. However, there is difficult to obtain data about gas turbine transient response for step in fuel or load.

The model of the gas turbine system is a simple model structure for gas turbine transient behaviour from fuel input to power output. The model time response can easily be modified by adjusting volume sizes (burner volume and volume between gas turbines) and shaft inertias. Also note that gas turbine power is

independent of turbine speed. The step responses in Figure 4.13 show that the gas turbine can be modeled with first order step response.

6 Conclusions

6.1 Conclusions

The aim of this thesis was to develop a compressor system model for anti-surge control validation. The model was developed using *Reynolds transport theorem* and control volume analysis, the law of conservation of angular momentum and compressor experimental characteristics. The model was implemented in Simulink® and identified and validated against experimental data from an oil and gas installation.

Simulations showed that the final model gave a good fit to the experimental values. Observations indicated that the compressor system dynamics are dominated by large volumes, mainly upstream and downstream systems, and compressor characteristics. The recycle valve size and characteristics is also essential for anti surge control validations. Dynamics in smaller volumes in the compressor system are damped out by the large volumes, and flow dynamics in ducts are also damped out.

6.2 Future work

It still remains some validation work on the model. One of the challenges are limitations in available process data. More flow measurement in the process would simplify the validation. To compensate for this, the model can be extended to include both the first and second stage compressor. This will give a better model of the second stage compressor system inlet conditions. The model should also be validated for larger variations in the compressor inlet temperature.

To easier be able to study surge margins, the compressor transient should be drawn onto a compressor chart. This would allow us to observe weather the transient response somewhere is too close to the surge line and therefore identify critical phases of surge avoidance control.

The proposed model does not take multiphase flow into account. A possible extension is to include the gas composition in the model and use a phase diagram to determine how much liquid is drained in the scrubber. This extension will allow us to have different mole weight in the different modules. This will also allow us to study how different gas composition can affect the system regarding surge.

The specific heats used in the model are static values. For modules where the variation in temperature is large, the specific heat for the average temperature

is used. The model can be extended to take varying specific heat into account.

These are just a few of many possible extensions and improvements to the model. Before putting an effort in improving the model, one should always consider weather the improvement will be significant for the model and if it will reduce the gap between the model and the real system.

7 References

Air Liquide Encyclopaedia (2009), Web.
http://encyclopedia.airliquide.com/encyclopedia.asp.

Balchen, J. G., Andresen, T. and Foss, B. A. (2003), *Reguleringsteknikk*, Institutt for teknisk kybernetikk.

Bøhagen, B. (2007), Active surge control of centrifugal compression systems, PhD thesis, NTNU.

Bossel, U. (2003), 'Well-to-wheel studies, heating values, and the energy conservation principle'.

Camporeale, S. M., Fortunato, B. and Mastrovito, M. (2006), 'A modular code for real time dynamic simulation of gas turbines in simulink', *Journal of Engineering for Gas Turbines and Power* **128**(3), 506–517.
http://link.aip.org/link/?GTP/128/506/1.

Cohen, H., Rogers, G. and Saravanamuttoo, H. (1996), *Gas turbine theory*, 4th edn, Addison Wesley Longman Limited.

Egeland, O. and Gravdahl, J. T. (2002), *Modeling and Simulation for Automatic Control*, Marine Cybernetics.

Engineering toolbox (2009), Web.
http://www.engineeringtoolbox.com.

Gravdahl, J. T. (2001), Loadsharing using temperature for centrifugal compressors on a common shaft. NTNU-Dept. of Engineering Cybernetics / ABB Industri AS.

Gravdahl, J. T. and Egeland, O. (1998), *Compressor surge and rotating stall*, Springer.

Kim, J. H., Song, T. W., Kim, T. S. and Ro, S. T. (2001), 'Model development and simulation of transient behavior of heavy duty gas turbines', *Journal of Engineering for Gas Turbines and Power* **123**(3), 589–594.
http://link.aip.org/link/?GTP/123/589/1.

Moran, M. J. and Shapiro, H. N. (2000), *Fundamentals of engineering thermodynamics*, John Wiley & Sons, Inc.

Morini, M., Pinelli, M. and Venturini, M. (2007), 'Development of a one-dimensional modular dynamic model for the simulation of surge in compression systems', *Journal of Turbomachinery* **129**(3), 437–447. http://link.aip.org/link/?JTM/129/437/1.

Reed, J. A. (1993), Java gas turbine simulator: Engine component mathematical models. Summary of Master of Sciency thesis "Development of an Interactive Graphical Aircraft Propulsion System Simulator".

Skogestad, S. (2000), *Prosessteknikk, Masse- og energibalanser*, Tapir akademisk forlag.

Smith, R. C. (2009), 'Statistical validation of scientific models', Web. http://www4.ncsu.edu/∼rsmith/MA797V_S08/Lecture12.pdf.

Spirax Sarco, Pipes and pipe sizing (2009), Web. http://www.spiraxsarco.com/resources/steam-engineering-tutorials/steam-distribution/pipes-and-pipe-sizing.asp.

Venturini, M. (2005), 'Development and experimental validation of a compressor dynamic model', *Journal of Turbomachinery* **127**(3), 599–608. http://link.aip.org/link/?JTM/127/599/1.

White, F. M. (1999), *Fluid mechanics*, fourth edition edn, McGraw Hill.

Appendix A Simulink model

The attached zip-file contains the Simulink® implementation of the compressor system and the gas turbine system:

- *readme.txt* contains a brief description of the model files.
- *Compressor system* (folder) contains the compressor system model.
- *Gas turbine system* (folder) contains the gas turbine system model.

Appendix B Mass, momentum and energy balance

B.1 Mass balance

For a control volume (fixed or deforming) with one-dimensional flux terms we have

$$\left(\frac{\mathrm{d}m}{dt}\right)_{syst} = \frac{\mathrm{d}}{dt}\left(\int_{CV} \rho \, dV\right) + \sum_i (\rho_i A_i C_i)_{out} - \sum_i (\rho_i A_i C_i)_{in} = 0.$$

where CV denotes the control volume. Rearranging the equation gives

$$\begin{aligned}\frac{\mathrm{d}}{dt}\left(\int_{CV} \rho \, dV\right) &= \sum_i (\rho_i A_i C_i)_{in} - \sum_i (\rho_i A_i C_i)_{out} \\ &= w_{in} - w_{out},\end{aligned}$$

where the subscripts in and out denotes flows in and out of the control volume shich are summed up to inlcude all inlets and outlets. For a fixed control volume we have

$$\frac{\mathrm{d}}{dt}\left(\int_{CV} \rho \, dV\right) = \int_{CV} \frac{\partial \rho}{\partial t} \, dV = \frac{\mathrm{d}m}{dt} = w_{in} - w_{out}. \tag{B.1}$$

B.2 Momentum balance

For a control volume (fixed or deforming) with one-dimensional flux terms we have

$$\frac{\mathrm{d}}{dt}(m\vec{C})_{syst} = \sum \vec{F} = \frac{\mathrm{d}}{dt}\left(\int_{CV} \rho \vec{C} \, dV\right) + \sum_i (\dot{m}_i \vec{C}_i)_{out} - \sum_i (\dot{m}_i \vec{C}_i)_{in}, \tag{B.2}$$

where $\dot{m}_i$ denotes mass flow rate over an inlet or outlet, and $\vec{C}_i$ its velocity vector.

B.3 Energy balance

For a fixed control volume we have

$$\frac{\mathrm{d}Q}{dt} - \frac{\mathrm{d}W}{dt} = \frac{\mathrm{d}E}{dt} = \frac{v}{dt}\left(\int_{CV} e\rho \, dV\right) + \int_{CS} e\rho(\vec{C} \cdot \vec{n}) \, dA,$$

where CV denotes the control volume, and CS its surface. The velocity vector at the surface is denoted $\vec{C}$ and $\vec{n}$ is a unit vector perpendicular to the control

volume surface pointing outwards such that $\vec{C} \cdot \vec{n}$ is positive of flows leaving the control volume, and negative for flows entering the volume. Recall that positive Q denotes heat added to the system, while positive W denotes work done by the system. The system energy per unit is $e = e_{internal} + e_{kinetic} + e_{potential} + e_{other}$ where e_{other} represents effects like chemical reactions, nuclear reactions etc. which can be neglected in this case.For one-dimensional flux terms we have

$$\dot{Q} - \dot{W} = \frac{\partial}{\partial t}\left[\int_{CV}\left(u + \frac{1}{2}C^2 + gz\right)\rho\, dV\right] + \int_{CS}\left(h + \frac{1}{2}C^2 + gz\right)\rho(\vec{C}\vec{n})\, dA.$$

For a control volume with a series of one-dimensional inlets and outlets, the surface integral reduces and we get

$$\dot{Q} - \dot{W} = \frac{\partial}{\partial t}\left[\int_{CV}\left(u + \frac{1}{2}C^2 + gz\right)\rho\, dV\right] + \sum\left(h + \frac{1}{2}C^2 + gz\right)_{out}\dot{m}_{out} - \sum\left(h + \frac{1}{2}C^2 + gz\right)_{in}\dot{m}_{in}. \quad \text{(B.3)}$$

Appendix C Thermodynamic notions and values

C.1 Isothermal process

In an isothermal process the temperature stays constant. This is typically occurs for systems in contact with an outside thermal reservoir that changes slow enough to allow the system to adjust to the outside temperature through heat exchange. Using ideal gas model we see that $pV = constant$ for an isothermal process when the flow in and out of the system is zero.

C.2 Isobaric process

In an isobaric process the pressure stays constant. When heat is transferred to a system, the heat transferred will both do work on the environment and change the internal energy of the system.

C.3 Isochoric process

In a isochoric process the volume is held constant, which implies that the process doen no work on the environment.

C.4 Adiabatic process

In an adiabatic process there is no heat transfer with the environment. If the process also is reversible, it is called isentropic. For an adiabatic process $pV^{\kappa} = constant$.

The following adiabatic relation will be used in this thesis:

$$\frac{T_2}{T_1} = \left(\frac{p_2}{p_1}\right)^{\frac{\kappa-1}{\kappa}} \tag{C.1}$$

C.5 Polytropic process

For a polytropic process $pV^n = constant$ where $1 < n < \kappa$. Processes which are not purely isothermal or adiabatic can be characterized as polytropic. We have $n = 0$ for isobaric processes, $n = 1$ for isothermal, $n = \kappa$ for adiabatic and $n = \infty$ for isochoric.

C.6 Specific heat values

The table shows specific heat values for air at different temperatures (Moran and Shapiro, 2000, p. 838).

Temp $[K]$	c_p	κ
250	1.003	1.401
300	1.005	1.400
350	1.008	1.398
400	1.013	1.395
450	1.020	1.391
500	1.029	1.387
550	1.040	1.381
600	1.051	1.376
650	1.063	1.370
700	1.075	1.364
750	1.087	1.359
800	1.099	1.354
900	1.121	1.344
1000	1.142	1.336

C.7 Isentropic and polytropic efficiency

Efficiency for compressors and gas turbines can be defined in two ways, isentropic and polytropic. Both of them are described in detail in Cohen et al. (1996, p. 48-53).

Isentropic efficiency For compressor isentropic efficiency yield

$$T_2 - T_1 = \frac{T_1}{\eta_c}\left[\left(\frac{p_2}{p_1}\right)^{\frac{\kappa-1}{\kappa}} - 1\right], \tag{C.2}$$

where the subscripts 1 and 2 denotes the inlet and the outlet respectively, and η_c the isentropic efficiency.

Equivalent for gas turbines are

$$T_1 - T_2 = \eta_t T_1\left[1 - \left(\frac{p_2}{p_1}\right)^{\frac{\kappa-1}{\kappa}}\right]. \tag{C.3}$$

Polytropic efficiency Using polytroic efficiency for compressors gives

$$\frac{T_2}{T_1} = \left(\frac{p_2}{p_1}\right)^{\frac{\kappa-1}{\kappa\eta_{\infty c}}}, \tag{C.4}$$

where the subscripts 1 and 2 denotes the inlet and the outlet respectively, and $\eta_{\infty c}$ the polytropic efficiency.

Equivalent for gas turbines are

$$\frac{T_1}{T_2} = \left(\frac{p_1}{p_2}\right)^{\frac{(\kappa-1)\eta_{\infty t}}{\kappa}}. \tag{C.5}$$

Appendix D Model identification plots

D.1 Cooler

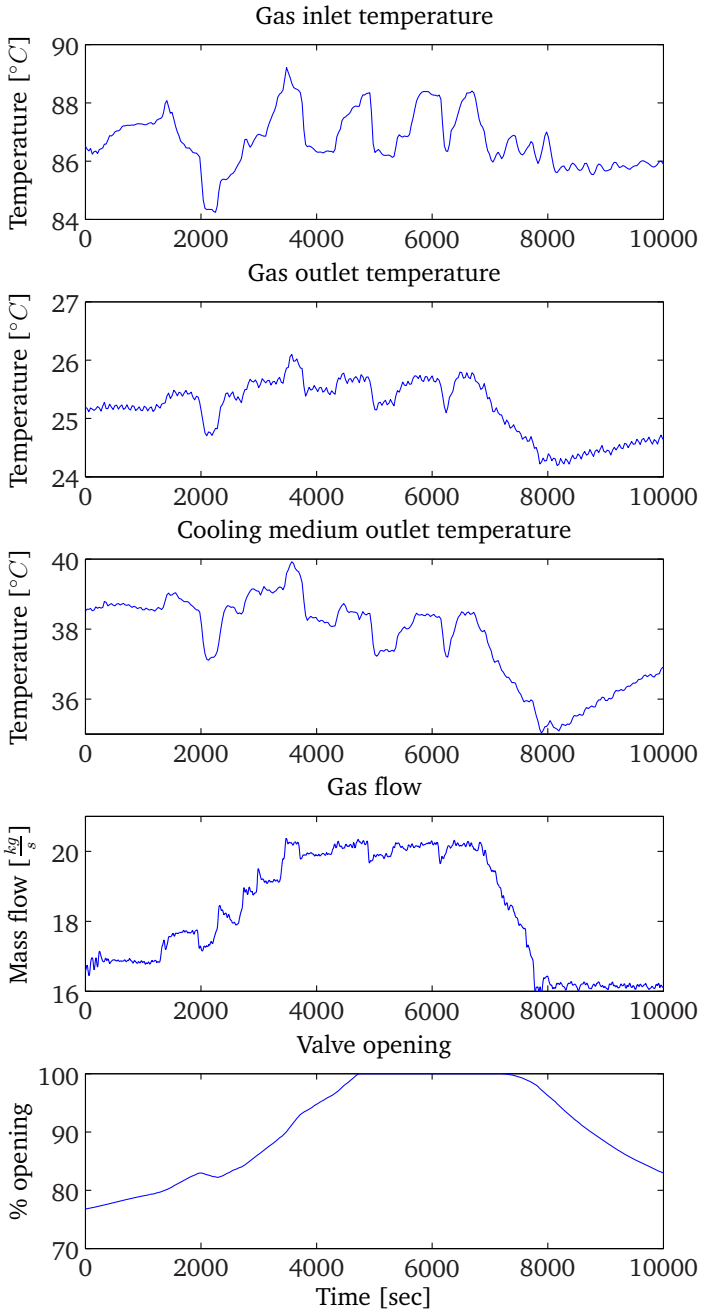

Figure D.1: Measured cooler input and outputs for full valve opening.

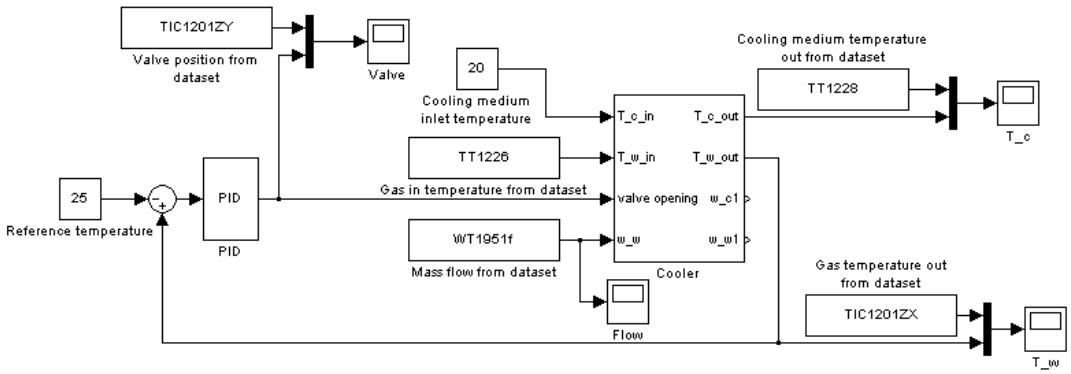

Figure D.2: Simulink test setup for cooler.

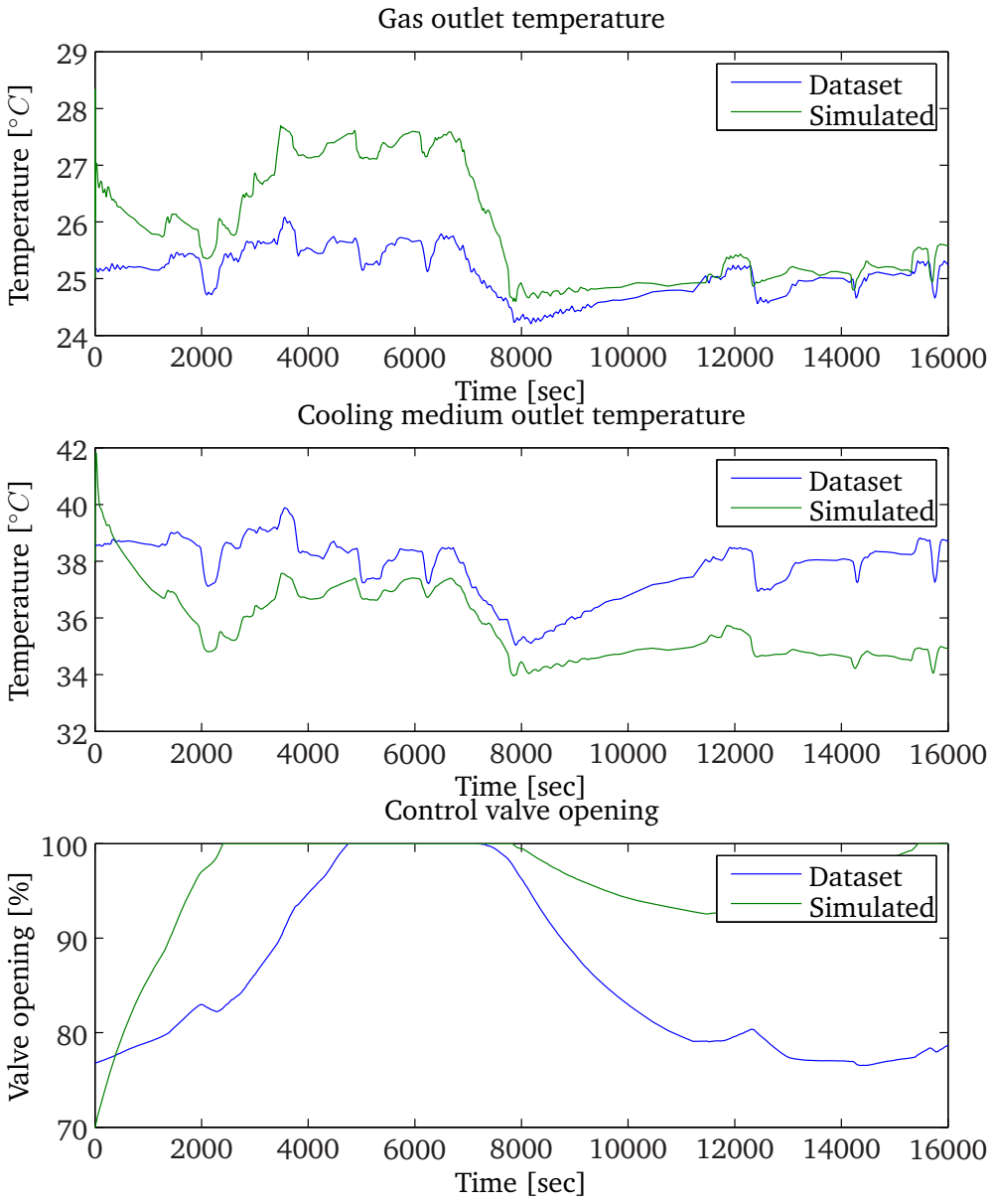

Figure D.3: Cooler closed loop verification for $n = 4$.

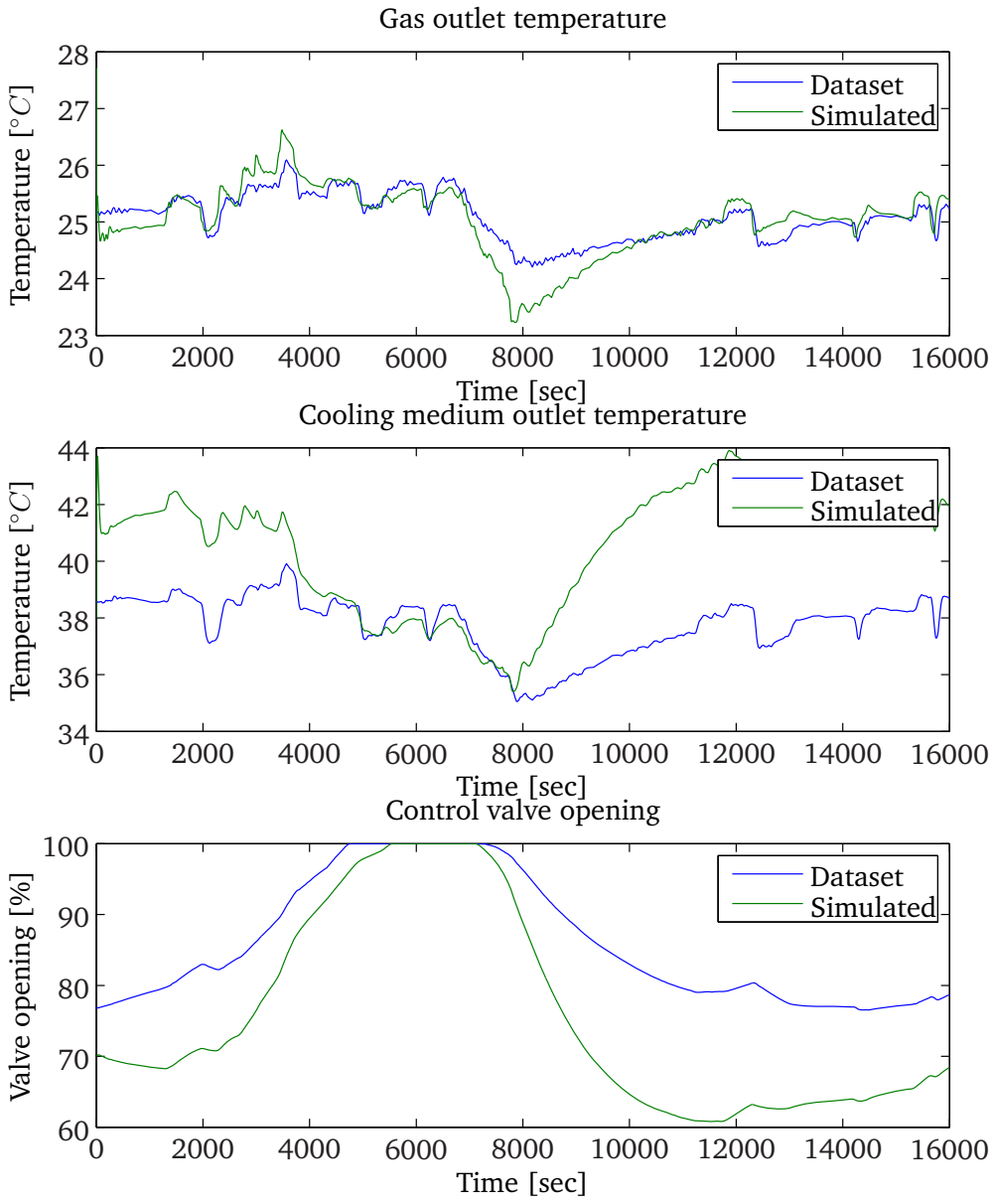

Figure D.4: Cooler closed loop verification for $n = 6$.

Appendix E Subscripts

Abbreviation	Description
c	Compressor including ducting and downstream volume.
cu	Compressor upstream.
cd	Compressor downstream.
uv	Upstream vessel to compressor system.
ud	Upstream duct between upstream vessel and manifold.
dv	Downstream vessel to compressor system.
m	Manifold merging upstream vessel and recycle line to cooler.
co	Cooler upstream compressor.
cm	Cooler cooling medium.
sc	Scrubber upstream compressor.
sp	Split from compressor to check valve and recycle line.
cv	Check valve between compressor outlet and downstream vessel.
rl	Recycle line with recycle valve.
sh	Shaft connecting compressor and governor.
g	Governor driving compressor.
i	Inlet to upstream vessel.
ct	Compressor including ducting in turbine system.
st	Shaft between compressor and gas turbine in gas generator.
cb	Combustor.
f	Fuel to combustor.
gt	Gas turbine.
vt	Volume between gas turbine and power turbine.
pt	Power turbine.
l	Load attached to power turbine.
a	Ambient conditions.